

Fig. 6. Kinetics of antigen deposition after FITC–OVA administration to HR-1 hairless mice via MN patch delivery, intradermal (ID) injection of reconstituted FITC–OVA, or ID injection of phosphate-buffered saline containing FITC–OVA. (A) Representative in vivo fluorescence imaging for antigen deposition from 4 mice for each group. Images were captured by the CRI Maestro EX system at the indicated time point after administration. Here, time 0 means the time of MN removal after 1-h application. (B) Integrated fluorescence intensity for the injection site as a function of time after administration. The intensity was measured from images captured using Maestro version 2.10 software. Data represent the average \pm standard deviation of 4 measurements each.

no sufficient margin for safety, which resulted in the use of an applicator for insertion. In commercial use, rapid mass vaccination and self-administration require robust needle strength to enable administration without special training or equipment. Thus, we believe that further improvement in needle strength is necessary.

Dissolution characteristics evaluation using ATRA MN patches provided a better understanding of the application time. Placebo or OVA MNs were sufficiently dissolved within 60 min (Matsuo et al., 2012b). ATRA MNs required a 120-min application time for sufficient dissolution. This longer application time may be because of the poor water solubility of ATRA. For further evaluation of dissolution characteristics, antigen diffusion and deposition were assessed using FITC–OVA. FITC–OVA administration using MN patches resulted in prolonged antigen deposition compared with ID administration via a hypodermic needle. Prolonged antigen deposition via MN patch administration might depend on the greater

viscosity of sodium hyaluronate than of the PBS solution. These observations are similar to the results of del Pilar Martín et al., that is, stainless steel MN vaccination of a Qdot-labeled influenza virus also resulted in prolonged antigen deposition in the skin for up to 7 days (del Pilar Martín et al., 2012), and they suggested that the prolonged deposition might be because of the large size of the inactivated virus antigen and the kinetics of antigen trafficking to the draining lymph nodes. In addition to roles as an immune stimulant, aluminum hydroxide adjuvant also contributes to antigen deposition. These findings will be a potential advantage of MN immunization; that is, prolonged antigen exposure to antigen-presenting cells leads to robust immune responses.

Chemical stability data revealed that ATRA MN patches packaged in heat-sealed aluminum laminated sachet are stable under refrigerated conditions (4 °C) for up to 24 weeks. It is well known that ATRA is not stable against light, heat, or oxidants. Various

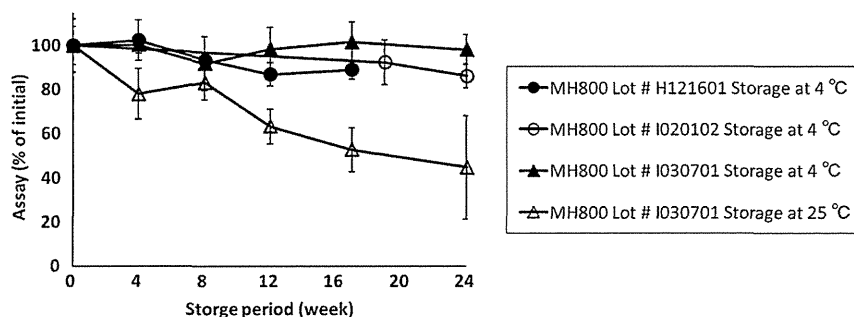


Fig. 7. ATRA stability as a function of storage time at 4 or 25 °C for ATRA-loaded MN patches. ATRA content was assayed by high-performance liquid chromatography. Data represent the average \pm standard deviation of 4 measurements each. Almost 15% drug loss was observed after storage at 4 °C for 24 weeks, but this loss was not significant (Student's *t*-test, $p = 0.08$). Conversely, approximately 50% loss was observed after 24 weeks at 25 °C (Student's *t*-test, $p < 0.05$).

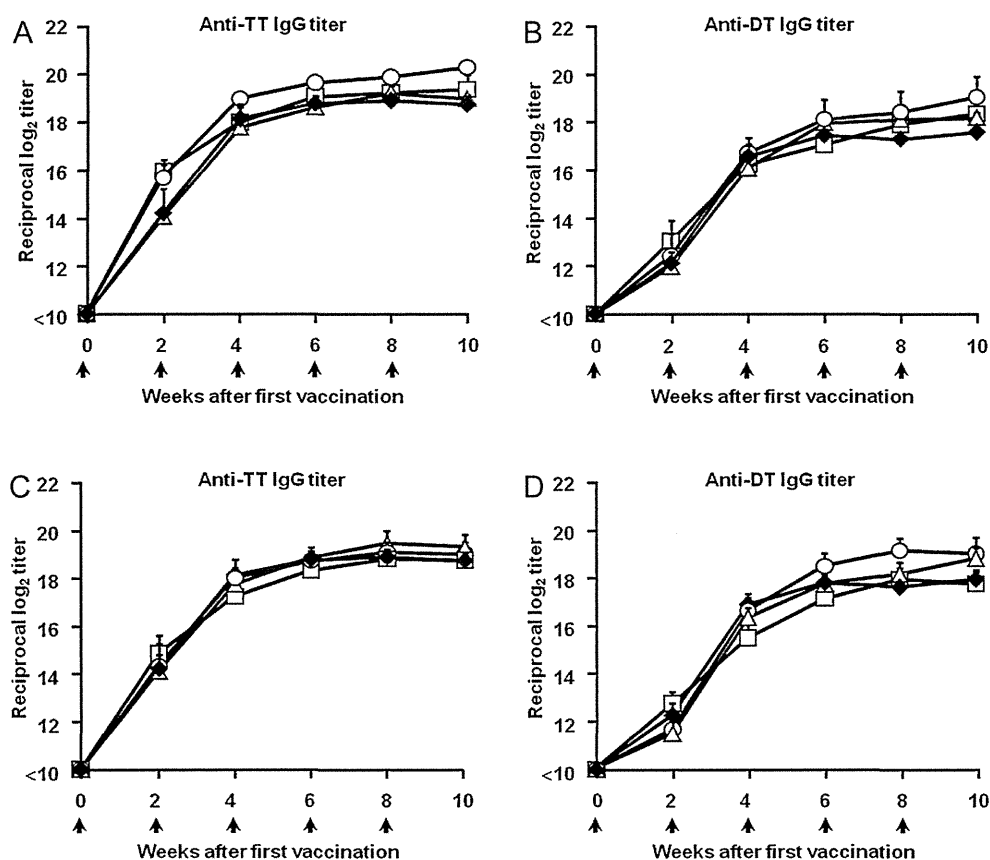


Fig. 8. Antigen-specific antibody responses after vaccination using MN patches (MH800) stored at various temperatures for 6 or 12 months. Combined tetanus toxoid (TT; 20 μ g) and diphtheria toxoid (DT; 10 μ g)-loaded MN patches stored at 4 °C (\circ), 25 °C (\square), 40 °C (\triangle) for (A) (B) 6 or (C–D) 12 months were pressed into the back skin of Wistar–ST rats. Vaccinations were repeated 5 times every 2 weeks. Arrows indicate the vaccination timing. As a control, freshly prepared combined TT (20 μ g) and DT (10 μ g)-loaded MN patches were also pressed into the back skin of Wistar–ST rats under the same vaccination schedule (\blacklozenge). At the indicated periods, sera were collected from the rats to determine the toxoid-specific IgG titers. Data are expressed as mean \pm standard error of 5 measurements.

formulations have been investigated (Brisaert et al., 1995; Hattori et al., 2012; Ozpolat and Lopez-Berestein, 2002; Zuccari et al., 2005). Lim et al. developed a solid lipid nanoparticle formulation to improve the stability, which exhibited good stability with more than 90% of the drug remaining after 1 month of storage at 4 °C. Our formulated ATRA MN patch also exhibited good stability after storage at 4 °C, with more than 90 and 85% of the drug remaining after 8 and 24 weeks of storage, respectively. The results indicated no significant incompatibility of the drug with the component materials of MicroHyal[®], sodium hyaluronate, dextran 70, and polyvidone. Because of the many therapeutic applications of ATRA, particularly in dermatological treatment, successful fabrication of ATRA MN patches allowed us to extend MN technology to both vaccination and novel therapeutic development in dermatology. As a proof of principle, we plan to investigate the feasibility of ATRA MN patches in the treatment of seborrheic keratosis, a common skin tumor.

Our study also demonstrated that MN patches stored at 40 °C for 12 months could induce robust antigen-specific immune responses comparable with those induced by freshly prepared MNs (Fig. 8). In addition to the immune response, the dissolution kinetics of TT/DT-loaded MNs was not changed by storage (Supplementary Fig. S2). Although further investigations using lower doses of vaccines or different types of vaccines are needed, the thermostabilities confirmed in this study suggest that MN vaccine formulations could be stored at room temperature, which would be an important benefit to increase vaccination coverage in developing countries where refrigeration is not sufficient.

5. Conclusion

This study evaluated the performance and characteristics of sodium hyaluronate-based MN patches to identify potential quality issues for future commercial usage. The advantage of prolonged antigen deposition after MN vaccination would lead to superior immune responses compared with those of traditional hypodermic needle vaccination. In addition, good stability without significant incompatibility with ATRA and TT/DT vaccines would permit the production of thermostable products. The ATRA MN patch will facilitate the development of new dermatological therapeutic applications. Overall, although its needle strength needs to be improved, our transcutaneous drug delivery system utilizing MicroHyal[®] would be an effective product for the simple, safe, and relatively painless delivery of drugs.

Acknowledgments

We acknowledge the Research Foundation for Microbial Diseases of Osaka University (Suita, Japan) for providing TT and DT, Kazuyuki Niki at Osaka University for help with the animal studies, and Tomomi Sato at Osaka University for assistance with fluorescence imaging by the CRi Maestro EX system. This work was supported by the Advanced Research for Medical Products Mining Programme of the National Institute of Biomedical Innovation (NIBIO); by Health and Labour Sciences Research Grants in Research on New Drug Development from the Ministry of Health, Labour, and Welfare; and by a Grant-in-Aid for Scientific Research (B)

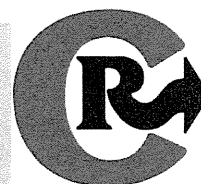
(24390041) from the Ministry of Education, Culture, Sports, Science, and Technology of Japan.

Appendix A. Supplementary data

Supplementary data associated with this article can be found, in the online version, at <http://dx.doi.org/10.1016/j.ijpharm.2012.10.042>.

References

- Al-Zahrani, S., Zaric, M., McCrudden, C., Scott, C., Kissenpfennig, A., Donnelly, R.F., 2012. Microneedle-mediated vaccine delivery: harnessing cutaneous immunobiology to improve efficacy. *Expert Opin. Drug Deliv.* 9, 541–550.
- Ameri, M., Fan, S., Maa, Y.-F., 2010. Parathyroid hormone PTH(1-34) formulation that enables uniform coating on a novel transdermal microprojection delivery system. *Pharm. Res.* 27, 303–313.
- Andrianov, A.K., DeCollibus, D.P., Gillis, H.A., Kha, H.H., Marin, A., Prausnitz, M.R., Babiuk, L.A., Townsend, H., Mutwiri, G., 2009. Poly[di(carboxylatophenoxy)phosphazene] is a potent adjuvant for intradermal immunization. *Proc. Natl. Acad. Sci. U.S.A.* 106, 18936–18941.
- Arora, A., Prausnitz, M.R., Mitragotri, S., 2008. Micro-scale devices for transdermal drug delivery. *Int. J. Pharm.* 364, 227–236.
- Bell, K.N., Hogue, C.J.R., Manning, C., Kendal, A.P., 2001. Risk factors for improper vaccine storage and handling in private provider offices. *Pediatrics* 107, e100.
- Berhane, Y., Demissie, M., 2000. Cold chain status at immunisation centres in Ethiopia. *East Afr. Med. J.* 77, 476–479.
- Brisaert, M.G., Everaerts, I., Plaizier-Vercammen, J.A., 1995. Chemical stability of tretinoin in dermatological preparations. *Pharm. Acta Helv.* 70, 161–166.
- Cosman, F., Lane, N.E., Bolognese, M.A., Zanchetta, J.R., Garcia-Hernandez, P.A., Sees, K., Matriano, J.A., Gaumer, K., Daddona, P.E., 2010. Effect of transdermal teriparatide administration on bone mineral density in postmenopausal women. *J. Clin. Endocrinol. Metab.* 95, 151–158.
- Darlenski, R., Surber, C., Fluhr, J.W., 2010. Topical retinoids in the management of photodamaged skin: from theory to evidence-based practical approach. *Br. J. Dermatol.* 163, 1157–1165.
- del Pilar Martin, M., Weldon, W.C., Zarnitsyn, V.G., Koutsouanos, D.G., Akbari, H., Skountzou, I., Jacob, J., Prausnitz, M.R., Compans, R.W., 2012. Local response to microneedle-based influenza immunization in the skin. *MBio* 3 (2), <http://dx.doi.org/10.1128/mBio.00012-12>, e00012–12.
- Didja, A., Darrouzet, H., Duchêne, D., Poelman, M.-C., 1989. Inclusion of retinoic acid in β -cyclodextrin. *Int. J. Pharm.* 54, 175–179.
- Gill, H.S., Denson, D.D., Burris, B.A., Prausnitz, M.R., 2008. Effect of microneedle design on pain in human volunteers. *Clin. J. Pain* 24, 585–594, [510.1097/AJP.1090b1013e31816778f31816779](http://dx.doi.org/10.1097/AJP.1090b1013e31816778f31816779).
- Gill, H.S., Prausnitz, M.R., 2007. Coating formulations for microneedles. *Pharm. Res.* 24, 1369–1380.
- Hattori, M., Shimizu, K., Katsumura, K., Oku, H., Sano, Y., Matsumoto, K., Yamaguchi, Y., Ikeda, T., 2012. Effects of all-trans retinoic acid nanoparticles on corneal epithelial wound healing. *Graefes Arch. Clin. Exp. Ophthalmol.* 250, 557–563.
- Heidemann, D., Jarosz, P., 1991. Preformulation studies involving moisture uptake in solid dosage forms. *Pharm. Res.* 8, 292–297.
- Hiraishi, Y., Nandakumar, S., Choi, S.-O., Lee, J.W., Kim, Y.-C., Posey, J.E., Sable, S.B., Prausnitz, M.R., 2011. Bacillus Calmette–Guérin vaccination using a microneedle patch. *Vaccine* 29, 2626–2636.
- Kim, Y.-C., Park, J.-H., Prausnitz, M.R., 2012a. Microneedles for drug and vaccine delivery. *Adv. Drug Deliv. Rev.*, <http://dx.doi.org/10.1016/j.addr.2012.04.005>.
- Kim, Y.C., Song, J.M., Lipatov, A.S., Choi, S.O., Lee, J.W., Donis, R.O., Compans, R.W., Kang, S.M., Prausnitz, M.R., 2012b. Increased immunogenicity of avian influenza DNA vaccine delivered to the skin using a microneedle patch. *Eur. J. Pharm. Biopharm.* 81, 239–247.
- Kis, E.E., Winter, G., Myschik, J., 2012. Devices for intradermal vaccination. *Vaccine* 30, 523–538.
- Kopp, S., 2006. Stability testing of pharmaceutical products in a global environment. *RAJ Pharma* <http://apps.who.int/medicinedocs/en/m/abstract/js19134en/>
- Lee, J.W., Park, J.H., Prausnitz, M.R., 2008. Dissolving microneedles for transdermal drug delivery. *Biomaterials* 29, 2113–2124.
- Lim, S.-J., Lee, M.-K., Kim, C.-K., 2004. Altered chemical and biological activities of all-trans retinoic acid incorporated in solid lipid nanoparticle powders. *J. Control. Release* 100, 53–61.
- Matsuo, K., Hirobe, S., Yokota, Y., Ayabe, Y., Seto, M., Quan, Y.-S., Kamiyama, F., Tougan, T., Horii, T., Mukai, Y., Okada, N., Nakagawa, S., 2012a. Transcutaneous immunization using a dissolving microneedle array protects against tetanus, diphtheria, malaria, and influenza. *J. Control. Release* 160, 495–501.
- Matsuo, K., Ishii, Y., Quan, Y.-S., Kamiyama, F., Mukai, Y., Yoshioka, Y., Okada, N., Nakagawa, S., 2011. Transcutaneous vaccination using a hydrogel patch induces effective immune responses to tetanus and diphtheria toxoid in hairless rat. *J. Control. Release* 149, 15–20.
- Matsuo, K., Yokota, Y., Zhai, Y., Quan, Y.-S., Kamiyama, F., Mukai, Y., Okada, N., Nakagawa, S., 2012b. A low-invasive and effective transcutaneous immunization system using a novel dissolving microneedle array for soluble and particulate antigens. *J. Control. Release* 161, 10–17.
- Ozpolat, B., Lopez-Berestein, C., 2002. Liposomal-all-trans-retinoic acid in treatment of acute promyelocytic leukemia. *Leuk. Lymphoma* 43, 933–941.
- Park, J.H., Allen, M.G., Prausnitz, M.R., 2005. Biodegradable polymer microneedles: fabrication, mechanics and transdermal drug delivery. *J. Control. Release* 104, 51–66.
- Prausnitz, M.R., 2004. Microneedles for transdermal drug delivery. *Adv. Drug Deliv. Rev.* 56, 581–587.
- Prausnitz, M.R., Langer, R., 2008. Transdermal drug delivery. *Nat. Biotechnol.* 26, 1261–1268.
- Prausnitz, M.R., Mikszta, J.A., Cormier, M., Andrianov, A.K., 2009. Microneedle-based vaccines. *Curr. Top. Microbiol. Immunol.* 333, 369–393.
- Quan, F.S., Kim, Y.C., Vunnavala, A., Yoo, D.G., Song, J.M., Prausnitz, M.R., Compans, R.W., Kang, S.M., 2010. Intradermal vaccination with influenza virus-like particles by using microneedles induces protection superior to that with intramuscular immunization. *J. Virol.* 84, 7760–7769.
- Skountzou, I., Quan, F.-S., Jacob, J., Compans, R.W., Kang, S.-M., 2006. Transcutaneous immunization with inactivated influenza virus induces protective immune responses. *Vaccine* 24, 6110–6119.
- Song, J.-M., Kim, Y.-C.O.E., Compans, R.W., Prausnitz, M.R., Kang, S.-M., 2012. DNA vaccination in the skin using microneedles improves protection against influenza. *Mol. Ther.* 20, 1472–1480.
- Sullivan, S.P., Koutsouanos, D.G., Del Pilar Martin, M., Lee, J.W., Zarnitsyn, V., Choi, S.O., Murthy, N., Compans, R.W., Skountzou, I., Prausnitz, M.R., 2010. Dissolving polymer microneedle patches for influenza vaccination. *Nat. Med.* 16, 915–920.
- Tas, C., Mansoor, S., Kalluri, H., Zarnitsyn, V.G., Choi, S.-O., Banga, A.K., Prausnitz, M.R., 2012. Delivery of salmon calcitonin using a microneedle patch. *Int. J. Pharm.* 423, 257–263.
- Tashtoush, B.M., Jacobson, E.L., Jacobson, M.K., 2007. A rapid HPLC method for simultaneous determination of tretinoin and isotretinoin in dermatological formulations. *J. Pharm. Biomed. Anal.* 43, 859–864.
- Young, J.F., 1967. Humidity control in the laboratory using salt solutions—a review. *J. Appl. Chem.* 17, 241–245.
- Zhu, Q.Y., Zarnitsyn, V.G., Ye, L., Wen, Z.Y., Gao, Y.L., Pan, L., Skountzou, I., Gill, H.S., Prausnitz, M.R., Yang, C.L., Compans, R.W., 2009. Immunization by vaccine-coated microneedle arrays protects against lethal influenza virus challenge. *Proc. Natl. Acad. Sci. U.S.A.* 106, 7968–7973.
- Zuccari, G., Carosio, R., Fini, A., Montaldo, P.G., Orienti, I., 2005. Modified polyvinylalcohol for encapsulation of all-trans-retinoic acid in polymeric micelles. *J. Control. Release* 103, 369–380.



A low-invasive and effective transcutaneous immunization system using a novel dissolving microneedle array for soluble and particulate antigens

Kazuhiko Matsuo ^a, Yayoi Yokota ^a, You Zhai ^a, Ying-Shu Quan ^b, Fumio Kamiyama ^b, Yohei Mukai ^a, Naoki Okada ^{a,*}, Shinsaku Nakagawa ^{a,**}

^a Department of Biotechnology and Therapeutics, Graduate School of Pharmaceutical Sciences, Osaka University, 1–6 Yamadaoka, Suita, Osaka 565–0871, Japan

^b CosMED Pharmaceuticals Co. Ltd, 448–5 Kajii-cho, Kamigyo-ku, Kyoto 602–0841, Japan

ARTICLE INFO

Article history:

Received 17 September 2011
Accepted 21 January 2012
Available online 28 January 2012

Keywords:

Dissolving microneedle array
Transcutaneous immunization
Vaccine
Skin
Soluble antigen
Particulate antigen

ABSTRACT

Transcutaneous immunization (TCI) is a promising needle-free, easy-to-use, and low-invasive vaccination method. The hydrogel patch-based TCI system induced immune responses against soluble antigens (Ags) like toxoids, but could not induce immune responses against particulate Ags. Here, as an effective TCI system against every form of Ag, we developed a dissolving microneedle array of three lengths (200, 300, or 800 μm) made of hyaluronate as a novel TCI device. Unlike conventional microneedles, the microneedles of our dissolving microneedle arrays dissolved in the skin after insertion. Each dissolving microneedle array effectively delivered both soluble and particulate Ags under the stratum corneum. TCI using these dissolving microneedle arrays induced effective immune responses in rats regardless of the Ag form that were comparable to conventional vaccination using subcutaneous immunization. In addition, application of these dissolving microneedle arrays caused only slight skin irritation. These findings suggest that our TCI system can simply, safely, and effectively improve protective immune responses for every vaccine Ag.

© 2012 Elsevier B.V. All rights reserved.

1. Introduction

Vaccination is the most effective preventive measure for protecting against infection-related mortality. Most vaccines are administered by injection with syringes and needles. Conventional injectable vaccination, however, has several inherent problems; the requirement for medical personnel or techniques, needle-related disease or injuries, and storage or transport issues, such as maintaining a proper cold chain [1,2]. These factors prevent the widespread use of vaccines in developing countries and rapid mass vaccination on an emergency basis, such as during an emerging pandemic. The development of easy-to-use, needle-free, and low-invasive vaccination methods is an urgent task globally.

Abbreviations: Ad, adenovirus vector; Ag, antigen; APC, antigen-presenting cell; DC, dendritic cell; dDC, dermal dendritic cell; ELISA, enzyme-linked immunosorbent assay; ELISPT, enzyme-linked immunospot; FITC, fluorescein isothiocyanate; HEK, human embryonic kidney; IDI, intradermal immunization; IFN, interferon; IL, interleukin; LC, Langerhans cell; OVA, ovalbumin; SCI, subcutaneous immunization; SP, silica particle; TCI, transcutaneous immunization; Th, helper T type; TS, tape-stripped.

* Correspondence to: N. Okada, Department of Biotechnology and Therapeutics, Graduate School of Pharmaceutical Sciences, Osaka University, 1–6 Yamadaoka, Suita, Osaka 565–0871, Japan. Tel.: +81 6 6879 8176; fax: +81 6 6879 8176.

** Correspondence to: S. Nakagawa, Department of Biotechnology and Therapeutics, Graduate School of Pharmaceutical Sciences, Osaka University, 1–6 Yamadaoka, Suita, Osaka 565–0871, Japan. Tel.: +81 6 6879 8175; fax: +81 6 6879 8179.

E-mail addresses: okada@phs.osaka-u.ac.jp (N. Okada), nakagawa@phs.osaka-u.ac.jp (S. Nakagawa).

Transcutaneous immunization (TCI) offers an attractive vaccination method as it has the advantage of improved compliance over conventional injection systems [3,4]. Skin, the target site of TCI, has an advanced immune system with antigen-presenting cells (APCs) such as Langerhans cells (LCs) or dermal dendritic cells (dDCs) [5–8]. Direct antigen (Ag) delivery to these APCs could enhance immune responses. The upper layer of the skin, the stratum corneum, consists of corneocytes embedded in a highly organized crystalline lamellar structure of the intercellular lipid matrix, thereby creating a physical barrier to substance penetration [9,10].

Previously, to overcome this barrier, we developed a hydrogel patch and revealed that a TCI system using the hydrogel patch induces effective immune responses against tetanus and diphtheria toxoids [11–13]. The hydrogel patch, however, less effectively promotes particulate and insoluble Ag penetration through the stratum corneum, thus TCI using a hydrogel patch does not induce effective immune responses against such Ags. Most practical vaccine Ags are in a particulate state, such as a less virulent strain of bacteria. The development of a different TCI system that is effective against all Ag forms is needed.

A microneedle array contains many micrometer-sized needles that can create a transport pathway large enough for proteins and nanoparticles, but small enough to avoid pain [14]. In addition, microneedle arrays have the advantage that they penetrate the stratum corneum barrier to target immunocompetent cells in the skin, and the use of a disposable array is suitable for self-administration by the patient

[15]. This is a promising approach for a TCI system to deliver various types of antigens into the skin. Gerstel and Place first presented a microneedle system in a 1976 patent [16]. The first paper to demonstrate the use of microneedles for transdermal delivery was not published until 1998 [17], but since then microneedle arrays made from silicon, metal, stainless steel, or titanium have been reported. The clinical use of microneedle arrays has faced serious obstacles because needles on microneedle arrays can fracture and remain in the skin, which is a safety issue. In 2004, however, microneedle systems made with biocompatible or biodegradable polymers began to be developed [18]. These systems are superior to conventional microneedle systems with regard to safety, leading to their early clinical use. Moreover, there are now several microneedle designs, such as solid microneedles, hollow microneedles, and coated microneedles. In the present study, we developed a dissolving microneedle array as a novel TCI device. Our dissolving microneedle array is made from sodium hyaluronate, as the base material. As sodium hyaluronate is a component of skin tissue, it is safe for exogenous material insertion. The needles inserted into the skin eventually dissolve because of their ability to retain water. Because skin characteristics differ between animal species, we conducted our experiments in both mice and rats. We first evaluated our dissolving microneedle array as a TCI device, and investigated its ability to induce immune responses using model Ags, ovalbumin (OVA) as model soluble Ags, and adenovirus vector (Ad) as model particulate Ags.

2. Materials and methods

2.1. Animals and cell line

Female C57BL/6 mice (6 weeks old), female BALB/c mice (6 weeks old), female hairless rats (5 weeks old), and female Wistar ST rats (5 weeks old) were purchased from SLC Inc. (Hamamatsu, Japan). All animals were maintained in the experimental animal facility at the Osaka University and experiments were conducted in accordance with the guidelines provided by the Animal Care and Use Committee of Osaka University.

Human embryonic kidney (HEK) 293 cells, the helper cell line for adenoviral vector (Ad) propagation, were purchased from American Type Culture Collection (Manassas, VA) and maintained in Dulbecco's modified Eagle's medium containing 10% fetal bovine serum.

2.2. Vector

Replication-deficient Ad was based on the adenovirus serotype 5 backbone with deletions of the E1 and E3 regions. Ad-Luc, which expresses firefly luciferase under control of the cytomegalovirus promoter, was previously constructed using an improved *in vitro* ligation method [19]. Ad-Luc was propagated in HEK293 cells, purified by two rounds of cesium chloride gradient ultracentrifugation, dialyzed, and stored at -80°C . Vector particle titers were evaluated spectrophotometrically using the method of Maizel et al. [20].

2.3. Hydrogel patch formulation

The hydrogel patch formulation was prepared as described previously [11–13]. The hydrogel patch formulation comprised cross-linked HiPAS™ acrylate medical adhesives (CosMED Pharmaceutical Co. Ltd., Kyoto, Japan): octyldodecyl lactate: glycerin: sodium hyaluronan = 100:45:30:0.2, as a weight ratio of composition.

2.4. Fabrication of dissolving microneedle arrays and vaccination procedure

The dissolving microneedle arrays containing Ags were fabricated by micromolding technologies with sodium hyaluronate as the base

material. Briefly, sodium hyaluronate was dissolved in distilled water, and then Ags were added and uniformly mixed. The aqueous solution was cast into micromolds and dried in a desiccator at room temperature. The dissolving microneedle arrays were obtained by separating them from the molds. The microneedle arrays contained over 200 microneedles/cm² that were 200, 300, or 800 μm long, each with a distance of 600 μm between them. To form the microneedle transcutaneous patch system, arrays with an area of 0.8 cm² were fixed onto an adhesive film with a surface area of 2.3 cm². Henceforth, we describe our dissolving microneedle array as the MicroHyla (MH) with a needle length of 200 μm (MH200), 300 μm (MH300), and 800 μm (MH800).

The vaccination procedure is shown in Supplementary Fig. 1. Forty-eight hours before application of each MH, the back skin of animals except hairless rats was shaved using clippers, exposed by removing hair with depilatory cream, washed with water, and dried. All MHs were pressed on skin using a handheld applicator at 12.8 N/200 microneedles.

2.5. Dissolution kinetics analysis of microneedles on each MH

The MH200, MH300, and MH800 were applied to back skin of BALB/c mice or Wistar ST rat for 5, 15, 30, or 60 min (Supplementary Fig. 1). After removing the MH, the microneedles of each MH were photographed using stereoscopic microscopy to measure the length of the remaining.

2.6. In vivo skin irritation study

The MH200, MH300, and MH800 were applied to the back skin of Wistar ST rat for 30 min. To estimate skin irritation by application of each MH, the test sites were observed and scored for the signs of erythema or edema according to the Draize dermal scoring criteria [21] at 5 min, and 2, 6, 24, 48, or 72 h after removing each MH. Furthermore, to evaluate the degree of skin barrier dysfunction, the skin surface impedance between the MH application area and the non-application skin area was measured within 30 s using a Pocket Tester (CDM-03D; Custom Inc., Kanagawa, Japan) 5, 15, 30, 60, or 120 min after removing each MH.

2.7. Substance delivery into the skin by each MH

After the application of each MH containing fluorescein isothiocyanate (FITC)-labeled ovalbumin (FITC-OVA; 1 μg) or FITC-labeled amorphous silica particles (FITC-SP, particle size diameter: 300 μm , COREFRONT Co., Ltd., Tokyo, Japan; 1×10^9 particle) for the indicated duration, the skin was harvested, embedded in OCT compound (Sakura Finetechnical Co., Ltd., Tokyo, Japan), and frozen in liquid nitrogen. Frozen sections (10- μm thick) were mounted with Prolong Gold antifade reagent with DAPI (Invitrogen, Carlsbad, CA), and then photographed using fluorescence microscopy (BZ-8000; Keyence Corporation, Osaka, Japan).

2.8. Vaccine protocol

To investigate the immune responses against (i) OVA (Sigma-Aldrich Inc., St. Louis, MO) as a model soluble Ag and (ii) Ad as a model particulate Ag, Wistar ST rats or hairless rats were vaccinated according to the following methods.

- (i) OVA (1 μg)-containing MH200, MH300, and MH800 were prepared. These were applied to the back skin of C57BL/6 mice or Wistar ST rats for 6 h. As subcutaneous immunization (SCI) or intradermal immunization (IDI) groups, C57BL/6 mice or Wistar ST rats were subcutaneously or intradermally injected with OVA (1 μg). This procedure was repeated four times every 2 weeks.

(ii) The Ad (7.7×10^9 virus particle)-containing MH800 was prepared. This was applied to the back skin of hairless rats for 6 h. As control groups, hairless rats were subcutaneously injected with Ad (7.7×10^9 virus particle), or transcutaneously immunized with OVA ($1 \mu\text{g}$) using a hydrogel patch. This procedure was repeated three times every 2 weeks.

The MH was covered with wound management film (BIOCLUSIVE; Johnson & Johnson Medical, Ltd., Tokyo, Japan) to allow for better skin adherence.

2.9. Antibody titer measurement

Serum was collected from immunized mice or rats at the indicated time points, and the Ag-specific IgG titer was determined by enzyme-linked immunosorbent assay (ELISA) following the previously described protocols [12]. End-point titers of the Ag-specific antibody were expressed as the reciprocal \log_2 of the last dilution that had 0.1 absorbance units after subtracting the background.

2.10. ELISPOT assay

C57BL/6 mice were transcutaneously, subcutaneously, or intradermally vaccinated with $100 \mu\text{g}$ OVA three times at 2-week intervals. Two weeks after the final vaccination, single-cell suspensions of lymph node cells or splenocytes were isolated from the mice and seeded onto 96-well plates at 4.0×10^5 cells/well. After 24-h stimulation with 1 mg/ml OVA, the frequency of interferon (IFN)- γ and interleukin (IL)-4-secreting cells specific for OVA was evaluated using a

mouse IFN- γ or IL-4 ELISPOT kit (Mabtech AB, Nacka Strand, Sweden) according to the manufacturer's protocol.

2.11. Inhibitory experiment for Ad infection

Two weeks after the final vaccination, hairless rats vaccinated three times with Ad were intravenously injected with Ad-Luc at vector particle titers of 10^9 . Two days later, the liver was removed from these hairless rats, weighed, and homogenized in phosphate-buffered saline containing $10 \mu\text{g/ml}$ aprotinin and $100 \mu\text{M}$ phenylmethylsulfonyl fluoride. Luciferase activity in the homogenates was determined using a luciferase assay system (Promega, Madison, WI).

3. Results

3.1. Fabrication and characteristics of each MH as a TCI device

We successfully fabricated three types of dissolving microneedle arrays made of sodium hyaluronate and in various forms and lengths: MH200, MH300, and MH800 (Fig. 1A). We examined the microneedles dissolution process at different times after skin insertion. For the MH200 and MH300 applied on both mice and rats, the microneedle tips dissolved within 5 min and were fully dissolved at 1 h (Fig. 1B,C). For the MH800, the microneedles were reduced in length by 50% within 5 min, and had completely dissolved by 1 h. These data showed microneedles surely dissolved in skin of animals with different thick stratum corneum. Thus, our TCI system using the MH should be applied for at least 1 h.

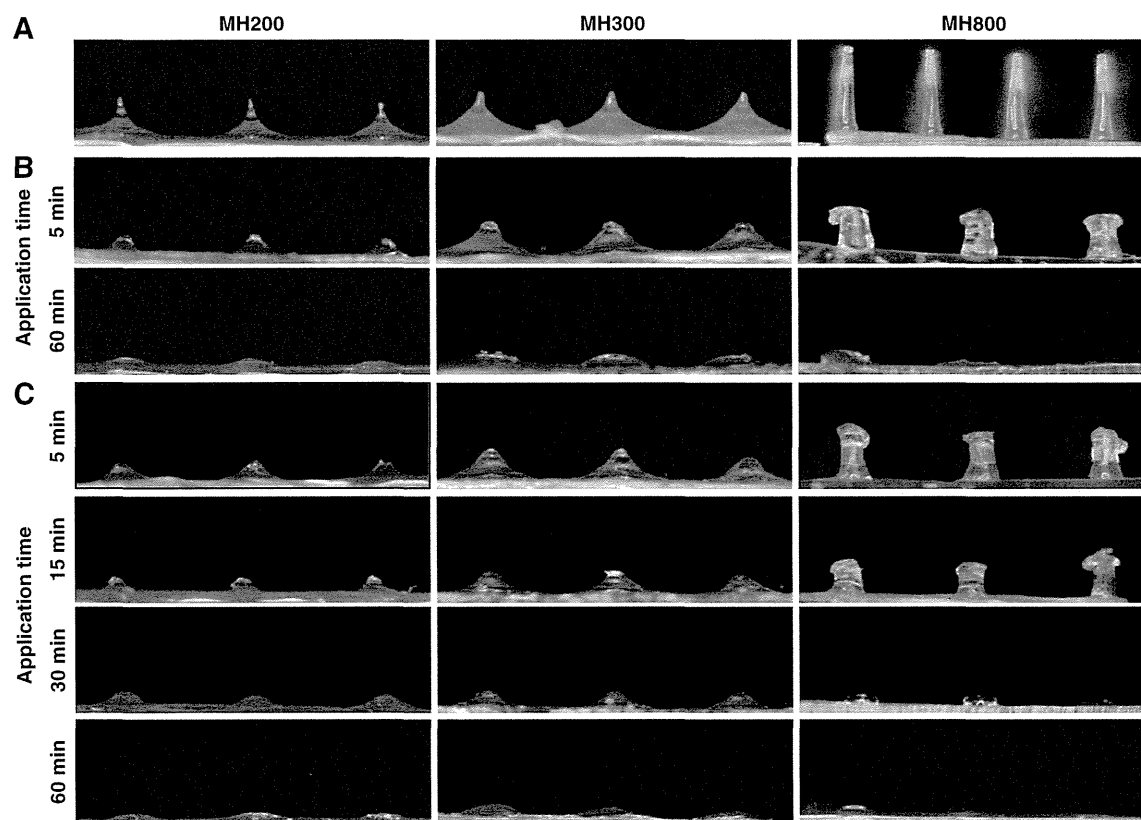


Fig. 1. Micrograph of dissolving microneedle arrays and dissolution kinetics of microneedles of each MH after skin insertion. (A) Bright-field micrograph of microneedles on MH200, MH300, and MH800. (B, C) The MH200, MH300, or MH800 was applied on the back skin of BALB/c mice (B) or Wistar ST rats (C) for 5, 15, 30, or 60 min. After removal of the MH, the microneedles remaining on each MH were photographed under a stereoscopic microscope.

3.2. Skin irritation caused by the application of each MH

We evaluated erythema and edema at the application site using the Draize scoring system after 30-min application of each MH (Fig. 2A). The skin of all rats showed no edema or erythema before application (data not shown). After 30 min application of each MH, edema was not observed in any rats. The MH800 induced slight or moderate erythema that gradually disappeared within a few days (Fig. 2B). The MH200 and MH300 induced slight erythema that disappeared within a few hours. In addition, we measured the skin impedance to evaluate the skin barrier dysfunction caused by each MH (Fig. 2C). Application of each MH decreased skin impedance immediately after removal: MH800 (20%) > MH200 (60%) > MH300 (70%), but these values recovered within 2 h. On the other hand, on tape-stripped skin in which the stratum corneum was physically removed, the relative skin electric impedance was decreased to 20% and did not recover within 2 h. This result suggests that the holes caused by insertion of each MH closed up quickly. Thus, application of each MH caused only temporary skin irritation, indicating that our dissolving microneedle arrays are low-invasive TCI devices.

3.3. Localization of antigens delivered by each MH

We evaluated whether the MH could deliver not only soluble Ags but also particulate Ags into the skin using FITC-OVA (soluble

substance) and FITC-SP (particulate substance). For mice, MH200 delivered FITC-OVA (green spot) or FITC-SP (green spot) into the epidermis and upper layer of the dermis, whereas MH300 and MH800 delivered them into mainly the dermis (Fig. 3A). On the other hand, for rats, MH200 and MH300 delivered FITC-OVA or FITC-SP into the epidermis and upper dermis layer, whereas MH800 delivered them from the epidermis to the lower dermis layer in the skin (Fig. 3B). These results indicated that the MH delivered various Ags into the skin regardless of the Ag form. In addition, the MH size can be used to control the Ag delivery site.

3.4. Characterization of immune responses induced by TCI using the Ag-encapsulating MHs

We investigated whether our TCI system using each MH induced Ag-specific IgG production against OVA as a model soluble Ag. TCI using each MH increased anti-OVA IgG titer in the sera of both C57BL/6 mice and Wistar ST rats (Fig. 4A,B). The effect tends to be equal or superior to that of SCI or IDI group. Additionally, in comparison of antibody production between TCI using MH200, MH300, and MH800, for C57BL/6 mice, anti-OVA IgG titer induced by TCI using MH300 or MH800 was higher than that of MH200 (Fig. 4a). On the other hand, Wistar ST rats vaccinated once with MH800 showed higher OVA-specific IgG production than that in the TCI

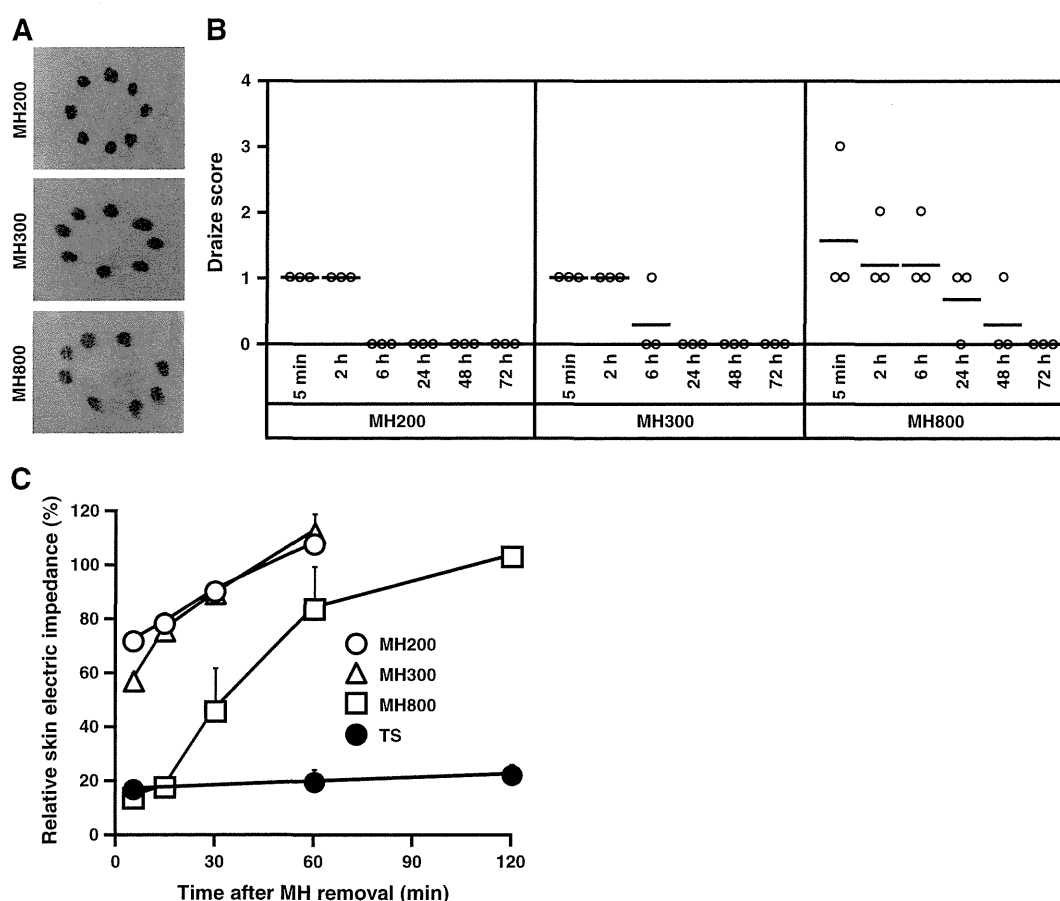


Fig. 2. Assessment of skin irritation caused by application of each MH. The MH200, MH300, or MH800 was applied to the back skin of Wistar ST rats for 30 min. (A) After MH removal, the application site was observed. (B) The degree of erythema on the skin of Wistar ST rats was scored using the Draize scoring system; 0, no erythema or edema; 1, very slight erythema and/or barely perceptible edema; 2, well-defined erythema and/or slight edema; 3, moderate to severe erythema or moderate edema, and 4, severe erythema and/or edema. Mean value is shown as a bar. (C) Skin impedance between the MH application area and non-application area was measured 5, 15, 30, 60, and 120 min after the removal of each MH. As the control group, the back skin of Wistar ST rats was tape-stripped. Data are expressed as mean \pm SE of results from three rats. TS, tape-stripped, TCI; transcutaneous immunization. In each section, the stratum corneum lies between the top line and the middle line, the living epidermis lies between the middle line and bottom line, and the dermis lies under the bottom line.

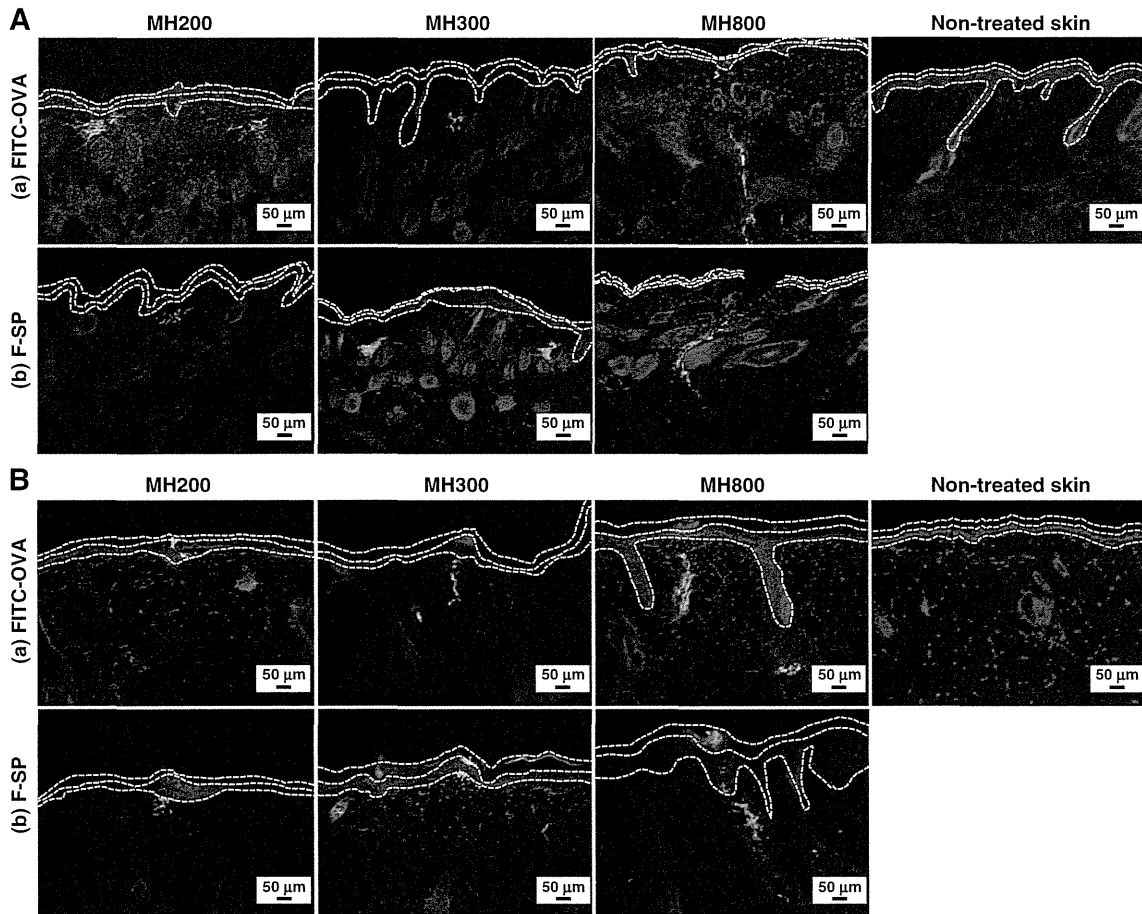


Fig. 3. Skin sections from animals vaccinated with each MH encapsulating FITC-OVA or FITC-SP. FITC-OVA (green) or FITC-SP (green)-containing MH200, MH300, and MH800 were applied on the back skin of C57BL/6 mice (A) or Wistar ST rats (B) for 6 h. The skin was harvested and frozen. Frozen sections (6- μ m thick) were photographed under a fluorescence microscope. The nucleus was counterstained using DAPI (blue).

groups using MH200 and MH300, but the anti-OVA IgG titer reached maximum levels by the fourth vaccination in all TCI groups (Fig. 4B).

To evaluate the Th1/Th2 balance in the immune responses induced by our TCI, we analyzed the OVA-specific IgG subclass. On the analysis of IgG subclass in C57BL/6 mice, OVA injection induced mainly anti-

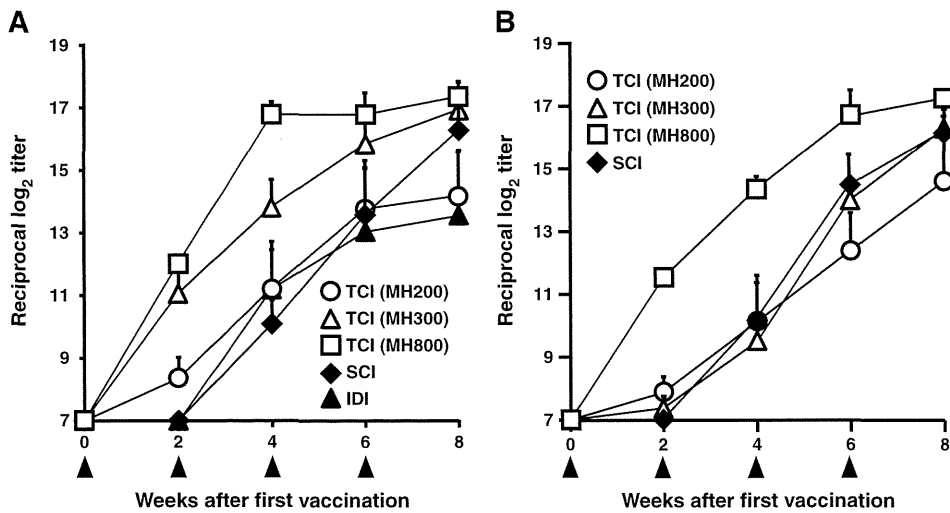


Fig. 4. OVA-specific antibody responses after transcutaneous vaccination. C57BL/6 mice (A) or Wistar ST rats (B) were transcutaneously vaccinated with 1 μ g OVA using MH200, MH300, or MH800 for 6 h four times at 2-week intervals. A control group was subcutaneously or intradermally immunized with 1 μ g OVA. At the indicated points, sera collected from these mice or rats were assayed for the OVA-specific IgG titer by ELISA. TCI; transcutaneous immunization, SCI; subcutaneous immunization, IDI; intradermal immunization. Arrowhead indicates vaccination point.

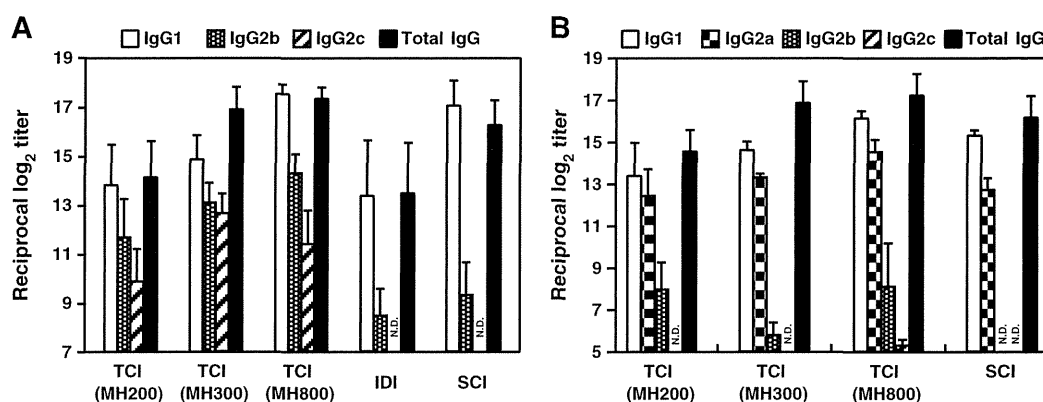


Fig. 5. Analysis of OVA-specific IgG subclass. An OVA (1 μ g)-encapsulated MH200, MH300, or MH800 were applied to the back skin of C57BL/6 mice (A) or Wistar ST rats (B) for 6 h four times at 2-week intervals. A control group was subcutaneously or intradermally immunized with 1 μ g OVA. Two weeks after the final vaccination, serum collected from these animals was assayed for OVA-specific IgG subclass (IgG1, IgG2a, IgG2b, IgG2c) titer by ELISA. Data are expressed as mean \pm SE of results from 5 animals. ND; not detectable, TCI; transcutaneous immunization, SCI; subcutaneous immunization, IDI; intradermal immunization.

OVA IgG subclass IgG1 (Th2-type IgG subclass) not IgG2c (Th1-type IgG subclass), whereas TCI using MH200, MH300, and MH800 induced both IgG1 and IgG2c specific for OVA (Fig. 5A). On the other hand, in Wistar ST rats vaccinated by TCI using each MH, mainly IgG1 and IgG2a (Th2-type subclass) not IgG2c (Th1-type subclass) were increased, as well as in SCI group (Fig. 5B). TCI using MHs induced distinct immune responses between C57BL/6 mice and Wistar ST rats. The cause of these results might require further investigation.

Since, in C57BL/6 mice, interferon (IFN)- γ (Th1-type cytokine) and interleukin (IL)-4 (Th2-type cytokine) induce a class switch to IgG1 and IgG2c, we analyzed IFN- γ and IL4-secreting lymphocyte cells upon stimulation of OVA. In ELISPOT assay, the frequency of IFN- γ -secreting cells and IL-4-secreting cells in both lymph node cells and splenocytes of C57BL/6 mice vaccinated with OVA by TCI using MH200, MH300, or

MH800 were detected fewer than that of SCI group (Fig. 6). This result contradicted above data of IgG subclass analysis. Since various immune events might contribute Th1/Th2 immune balance, to understand the characteristics of immune responses induced by TCI using each MH in detail, we need to investigate Ag-capturing APC subsets and the Ag-presenting function of the APC subsets.

3.5. Protective efficacy against particulate antigen by TCI using Ag-encapsulating MHs

Furthermore, to examine whether our TCI system induced immune responses against particulate Ags, we evaluated the vaccine efficacy of the TCI using the MH800 against Ad as a particulate model Ag (Fig. 7A). TCI using MH800 increased the Ad-specific IgG

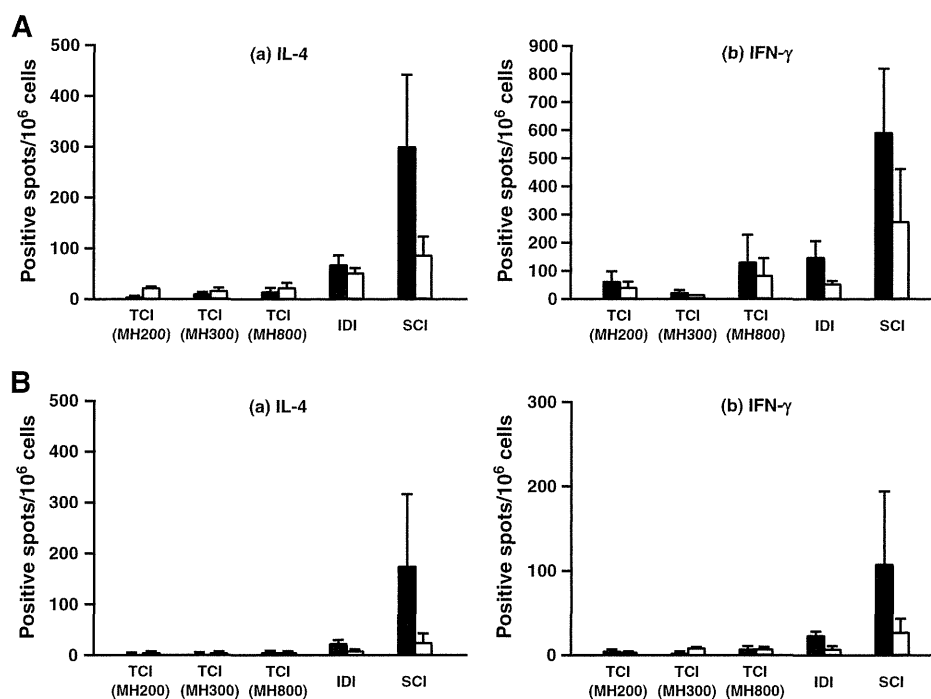


Fig. 6. Cytokine production in lymphoid tissue of mice vaccinated transcutaneously with OVA. C57BL/6 mice were transcutaneously vaccinated with 1 μ g OVA using MH200, MH300, or MH800 four times at 2-week intervals. As control groups, C57BL/6 mice were intradermally or subcutaneously immunized with 1 μ g OVA. Two weeks after the final vaccination, single-cell suspensions of draining lymph node cells (A) or splenocytes (B) were prepared and an ELISPOT assay was performed after stimulating the cells with (■) or without (□) 1 mg/ml OVA for 24 h. Data are expressed as mean \pm SE of results from five mice. TCI; transcutaneous immunization, SCI; subcutaneous immunization, IDI; intradermal immunization.

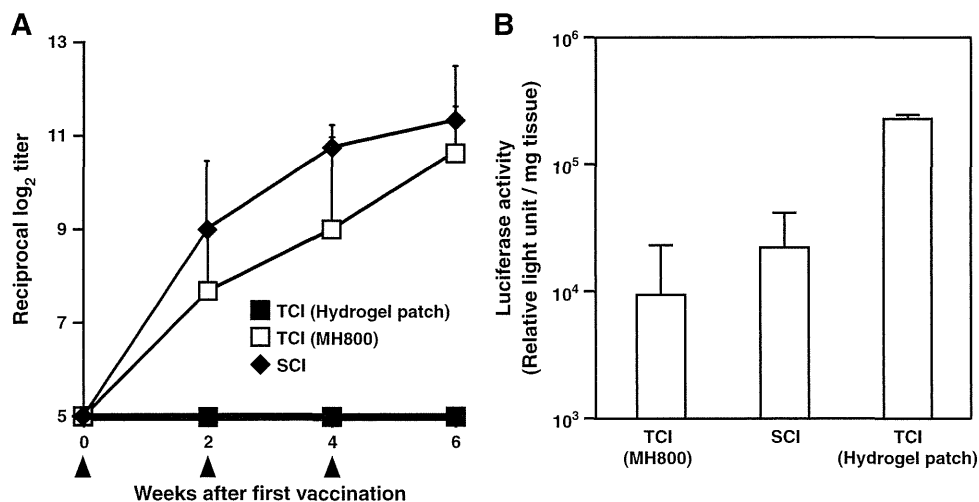


Fig. 7. Inhibitory effects for Ad infection in hairless rats vaccinated transcutaneously with Ad. Ad (7.7×10^9 VP) was applied on the back skin of hairless rats using an MH800 for 6 h, or using a hydrogel patch for 24 h at 2-week intervals. A control group was subcutaneously immunized with Ad (7.7×10^9 VP). (A) At the indicated points, sera collected from these rats were assayed for the Ad-specific IgG titer by ELISA. (B) Two weeks after the final vaccination, hairless rats vaccinated with Ad were intravenously injected with Ad-Luc at vector particle titers of 10^9 . Two days later, luciferase activity in liver homogenates was determined using a luciferase assay system. Data are expressed as mean \pm SE of 3 to 5 rats. Arrowheads indicate the vaccination point. TCI; transcutaneous immunization, SCI; subcutaneous immunization.

titer after the first vaccination. This effect was equal to that of the SCI group. On the other hand, hairless rats vaccinated with TCI using a hydrogel patch showed no Ad-specific IgG antibody production, because the hydrogel patch could not promote particulate Ag penetration through the stratum corneum. Next, to evaluate the neutralization activity of the anti-Ad IgG antibody, we intravenously injected into hairless rats 2 weeks after the final vaccination. Two days later, luciferase activity in the liver of hairless rats vaccinated transcutaneously using the MH800 was repressed compared with that of TCI using a hydrogel patch, comparable to that of the SCI group (Fig. 7B). Thus, TCI using the MH induced neutralizing antibodies against particulate antigens.

Based on these results, our TCI system using the MH induced immune responses against particulate Ags as well as soluble Ags, suggesting that our original device would be applicable to every type of vaccine Ag.

4. Discussion

In the present study, we developed our original TCI system using dissolving microneedle arrays; the MH made of sodium hyaluronate, which was fabricated in various forms and lengths; MH200, MH300, and MH800. The microneedles on the MH were dissolved by water in the skin and thus had no danger of remaining in the skin, making our MH safer than traditional microneedle arrays made of metal or stainless steel. In fact, the condition of the skin on which each MH was applied recovered immediately after MH removal.

In both animal species, mice and rats, each MH showed similar insertion characteristics and induction of immune response, suggesting that our MHs dissolved in the skin and delivered Ags into skin with various characteristics. Our results suggested that the MH can be developed for clinical use, because it will be suitable for insertion into people of different races with different skin characteristics all over the world. It is reported that the force required for the insertion of microneedles into skin is over 0.058 N/needle [18]. As the microneedles on each MH had enough force for insertion (data not shown), application to human skin is promising.

In addition, TCI using each MH induced Ag-specific immune responses. This result is due to the ability of Ag to be delivered by each MH into a living epidermis and dermis in which APCs are present. This is important information to advance the development of each MH. Human skin characteristics vary (skin thickness, skin turgor,

and so on) with those of rodent models, thus we are now investigating the characteristics of Ag delivery and microneedle insertion in a human skin model.

Furthermore, TCI using the each type of MH induced immune responses against both soluble and particulate Ags, suggesting that this system is applicable to not only soluble Ags like toxoids, but also to inactivated whole-organism vaccines and live vaccines. In this respect, further studies of the activity retention of Ags contained in the MH are needed.

In addition, there were difference in strength of Ag-specific antibody production induced by TCI using MH200, MH300, and MH800 in both mice and rats. This distinct immune response seemed to be due to differences in the APC subset involved in Ag capture. The APC subset differs in each layer of the skin, such as LCs in living epidermis [22] or dDC in dermis [23]. If Ags were delivered to different skin layers, then distinct immune responses would be induced. In mice, Ags administered into living epidermis and part of dermis by TCI using MH200 are captured mainly by LCs, whereas LCs as well as dDCs captured Ags delivered into both living epidermis and dermis by TCI using MH300 and MH800. On the other hand, in rats, Ags might be delivered into living epidermis and part of dermis by TCI using MH200 and MH300, and are thus captured mainly by LCs. Also, in rats vaccinated by TCI using MH800, LCs and dDCs capture Ags delivered into both living epidermis and dermis. Though the distinct immune function mechanism between LCs and dDCs is not completely clear, dDCs might migrate into regional lymph nodes more quickly than LCs in Ag administration [24]. We are currently working to identify the Ag-capturing APC subsets in TCI using each MH and to analyze the *in vivo* kinetics of these cells.

In addition, dDC were recently classified into two subsets; langerin (C-type lectin receptor; CD207)-positive dDC, or langerin-negative dDC [25–27]. The immune responses induced by these APC subsets in the skin, such as LC, langerin-positive dDC, or langerin-negative dDC, have not been investigated *in vivo*. Because the MH might deliver the Ags into particular skin layers, such as living epidermis and upper or lower layers of the dermis, the Ag can be selectively delivered to specific APC subsets, suggesting that it is possible to analyze the *in vivo* mechanism of immune function induced by these APC subsets. On the basis of these analyses, we will clarify the skin immune system and also discuss the detail immune characteristics of our TCI system. We are currently analyzing the association between Ag delivery site,

Ag-capturing cell groups, and immune responses by TCI using the MH200, MH300, and MH800.

5. Conclusion

These data indicated that our MH, as a novel TCI device, delivered Ags into the skin regardless of the Ag form. Therefore, TCI using the MH safely and effectively induced immune responses against soluble and particulate Ags. The application of our TCI system against practical infectious disease, such as influenza, is now being evaluated. In addition, we are currently working to analyze the mechanism of immune responses induced by our TCI.

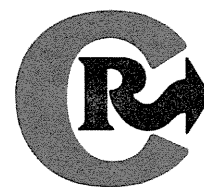
Supplementary materials related to this article can be found online at doi:10.1016/j.jconrel.2012.01.033.

Acknowledgments

This investigation was supported by the Program for the Promotion of Fundamental Studies in Health Sciences of the National Institute of Biomedical Innovation (NIBIO); a Grant-in-Aid for challenging Exploratory Research (No. 22659033) from the Ministry of Education, Culture, Sports, Science, and Technology of Japan; a Grant-in-Aid from The Uehara Memorial Foundation; a Grant-in-Aid from The Mochida Memorial Foundation for Medical and Pharmaceutical Research; and a Grant-in-Aid from the Tokyo Biochemical Research Foundation.

References

- [1] G. Kersten, H. Hirschberg, Needle-free vaccine delivery, *Expert Opin. Drug Deliv.* 4 (5) (2007) 459–474.
- [2] N. Azad, Y. Rojanasakul, Vaccine delivery-current trends and future, *Curr. Drug Deliv.* 3 (2) (2006) 137–146.
- [3] G.M. Glenn, D.C. Flyer, L.R. Ellingsworth, S.A. Frech, D.M. Frerichs, R.C. Seid, J. Yu, Transcutaneous immunization with heat-labile enterotoxin: development of a needle-free vaccine patch, *Expert Rev. Vaccines* 6 (5) (2007) 809–819.
- [4] T. Warger, H. Schild, G. Rechtsteiner, Initiation of adaptive immune responses by transcutaneous immunization, *Immunol. Lett.* 109 (1) (2007) 13–20.
- [5] A.R. Mathers, A.T. Larregina, Professional antigen-presenting cells of the skin, *Immunol. Res.* 36 (1–3) (2006) 127–136.
- [6] K. Sugita, K. Kabashima, K. Atarashi, T. Shimauchi, M. Kobayashi, Y. Tokura, Innate immunity mediated by epidermal keratinocytes promotes acquired immunity involving Langerhans cells and T cells in the skin, *Clin. Exp. Immunol.* 147 (1) (2007) 176–183.
- [7] C.L. Berger, J.G. Vasquez, J. Shofner, K. Mariwalla, R.L. Edelson, Langerhans cells: mediators of immunity and tolerance, *Int. J. Biochem. Cell Biol.* 38 (10) (2006) 1632–1636.
- [8] N. Romani, B.E. Clausen, P. Stoitzner, Langerhans cells and more: langerin-expressing dendritic cell subsets in the skin, *Immunol. Rev.* 234 (1) (2010) 120–141.
- [9] B.W. Barry, Breaching the skin's barrier to drugs, *Nat. Biotechnol.* 22 (2) (2004) 165–167.
- [10] J.M. Jensen, E. Proksch, The skin's barrier, *G. Ital. Dermatol. Venereol.* 144 (6) (2009) 689–700.
- [11] Y. Ishii, T. Nakae, F. Sakamoto, K. Matsuo, K. Matsuo, Y.S. Quen, F. Kamiyama, T. Fujita, A. Yamamoto, S. Nakagawa, N. Okada, A transcutaneous vaccination system using a hydrogel patch for viral and bacterial infection, *J. Control. Release* 131 (2) (2008) 113–120.
- [12] K. Matsuo, Y. Ishii, Y.S. Quen, F. Kamiyama, Y. Mukai, Y. Yoshioka, N. Okada, S. Nakagawa, Transcutaneous vaccination using a hydrogel patch induces effective immune responses to tetanus and diphtheria toxin in hairless rat, *J. Control. Release* 149 (1) (2011) 15–20.
- [13] K. Matsuo, Y. Ishii, Y.S. Quen, F. Kamiyama, Y. Mukai, Y. Yoshioka, N. Okada, S. Nakagawa, Characterization of transdermal delivery by a hydrogel patch in animals, human, and tissue-engineered skin model, *Biol. Pharm. Bull.* 34 (4) (2011) 586–589.
- [14] S. Henry, D.V. McAllister, M.G. Allen, M.R. Prausnitz, Microfabricated microneedles: a novel approach to transdermal drug delivery, *J. Pharm. Sci.* 88 (9) (1999) 948.
- [15] M.R. Prausnitz, Microneedles for transdermal drug delivery, *Adv. Drug Deliv. Rev.* 56 (5) (2004) 581–587.
- [16] M.S. Gerstel, V.A. Place, Drug Delivery Device, US Patent No. 3, 964 (1976) 482.
- [17] S. Henry, D.V. McAllister, M.G. Allen, M.R. Prausnitz, Microfabricated microneedles: a novel approach to transdermal drug delivery, *J. Pharm. Sci.* 87 (8) (1988) 922–925.
- [18] J.H. Park, M.G. Allen, M.R. Prausnitz, Biodegradable polymer microneedles: fabrication, mechanics and transdermal, drug delivery, *104 (1) (2005) 51–66.*
- [19] H. Mizuguchi, M.A. Kay, Efficient construction of a recombinant adenovirus vector by an improved in vitro ligation method, *Hum. Gene Ther.* 9 (17) (1998) 2577–2583.
- [20] J.V. Maizel Jr., D.O. White, M.D. Scharff, The polypeptides of adenovirus. I. Evidence for multiple protein components in the virion and a comparison of types 2, 7A, and 12, *Virology* 36 (1) (1968) 115–125.
- [21] J.H. Draize, G. Woodard, H.O. Calvery, Methods for the study of irritation and toxicity of substances applied topically to the skin and mucous membranes, *J. Pharmacol. Exp. Ther.* 82 (1944) 377–390.
- [22] N.C. Smith, L. Favila-Castillo, A. Monroy-Ostria, C. Hirunpetcharat, M.F. Good, The spleen, IgG antibody subsets and immunity to *Plasmodium berghei* in rats, *Immunol. Cell Biol.* 75 (3) (1997) 318–323.
- [23] D. Sen, L. Forrest, I. Parker, M.D. Cahalan, Selective and site-specific mobilization of dermal dendritic cells and Langerhans cells by Th1- and Th2-polarizing adjuvants, *Proc. Natl. Acad. Sci.* 107 (18) (2010) 8334–8339.
- [24] L.S. Bursch, L. Wang, B. Igyarto, A. Kissenpfennig, B. Malissen, D.H. Kaplan, K.A. Hogquist, Identification of a novel population of Langerin+ dendritic cells, *J. Exp. Med.* 204 (13) (2007) 3147–3156.
- [25] F. Ginhoux, M.P. Collin, M. Bogunovic, M. Abel, M. Leboeuf, J. Helft, J. Ochando, A. Kissenpfennig, B. Malissen, M. Grisotto, H. Snoeck, G. Randolph, M. Merad, Blood-derived dermal langerin+ dendritic cells survey the skin in the steady state, *J. Exp. Med.* 204 (13) (2007) 3133–3146.
- [26] L.F. Poulin, S. Henri, B. de Bovis, E. Devillard, A. Kissenpfennig, B. Malissen, The dermis contains langerin+ dendritic cells that develop and function independently of epidermal Langerhans cells, *J. Exp. Med.* 204 (13) (2007) 3119–3131.
- [27] M. Merad, F. Ginhoux, M. Collin, Origin, homeostasis and function of Langerhans cells and other langerin-expressing dendritic cells, *Nat. Rev. Immunol.* 8 (12) (2008) 935–947.



Transcutaneous immunization using a dissolving microneedle array protects against tetanus, diphtheria, malaria, and influenza

Kazuhiko Matsuo ^a, Sachiko Hirobe ^a, Yayoi Yokota ^a, Yurika Ayabe ^a, Masashi Seto ^a, Ying-Shu Quan ^b, Fumio Kamiyama ^b, Takahiro Tougan ^c, Toshihiro Horii ^c, Yohei Mukai ^a, Naoki Okada ^{a,*}, Shinsaku Nakagawa ^{a,**}

^a Laboratory of Biotechnology and Therapeutics, Graduate School of Pharmaceutical Sciences, Osaka University, 1-6 Yamadaoka, Suita, Osaka 565-0781, Japan

^b CosMED Pharmaceutical Co. Ltd., 32 Kawanishi-cho, Minami-ku, Kyoto 601-8014, Japan

^c Department of Molecular Protozoology, Research Institute for Microbial Diseases, Osaka University, 3-1 Yamadaoka, Suita, Osaka 565-0871, Japan

ARTICLE INFO

Article history:

Received 26 August 2011

Accepted 1 April 2012

Available online 11 April 2012

Keywords:

Dissolving microneedle array

Transcutaneous immunization

Tetanus

Diphtheria

Malaria

Influenza

ABSTRACT

Transcutaneous immunization (TCI) is an attractive alternative vaccination route compared to the commonly used injection systems. We previously developed a dissolving microneedle array for use as a TCI device, and reported that TCI with the dissolving microneedle array induced an immune response against model antigens. In the present study, we investigated the vaccination efficacy against tetanus and diphtheria, malaria, and influenza using this vaccination system. Our TCI system induced substantial increases in toxoid-specific IgG levels and toxin-neutralizing antibody titer and induced the production of anti-SE36 IgG, which could bind to malaria parasite. On influenza HA vaccination, robust antibody production was elicited in mice that provided complete protection against a subsequent influenza virus challenge. These findings demonstrate that TCI using a dissolving microneedle array can elicit large immune responses against infectious diseases. Based on these results, we are now preparing translational research for human clinical trials.

© 2012 Elsevier B.V. All rights reserved.

1. Introduction

Global epidemics of emerging infectious diseases such as highly pathogenic avian influenza [1,2] and the threatening reemergence of infectious diseases like malaria [3,4] are a major concern, emphasizing the importance of vaccination. Vaccination is the only fundamental prophylaxis against illness and death from infectious disease. The availability of novel vaccination methods is urgently needed at the outset of a pandemic or bioterrorism attack [5,6], because several problems are associated with conventional injectable vaccination systems, such as pain, requirement for medical personnel or techniques, needle-related disease or injuries, and storage and transportation issues.

Transcutaneous immunization (TCI) is a novel method that holds great potential for increasing the compliance and efficacy of future global vaccination programs [7,8]. A number of alternative strategies to delivering Antigens (Ags) into the skin, such as electroporation [9], iontophoresis

[10] and jet injector [11], are under investigation and some are undergoing clinical studies. Such approaches, however, require large-size and specific equipment to use for vaccination, or are accompanied by pain similar to standard injection systems. Some microneedle array designs have been developed [12], but most are made from metal or stainless steel, and some needles on microneedle arrays may fracture and remain in the skin, which is a safety issue. In comparison with these methods, dissolving microneedles offer several potential advantages [13]. First, this system is minimally invasive and has no need for needle disposal because the microneedles dissolve in the skin's interstitial fluid. These features might allay patient fears of needles and syringes, and also eliminate the risks of biohazardous sharps. Second, this system is simple and easy-to-use for vaccination. The use of a disposable array is suitable for self-administration by the patient. Third, this TCI system will likely cost much less than an injection system or other TCI system because the other methods require a cold chain for storage and transportation, such as TCI using a gauze patch that must be saturated with Ag solution just before application. In addition, clinical waste is eliminated because our microneedle array dissolves in the skin's interstitial fluid.

We developed dissolving microneedle arrays, called MicroHyal (MH), as a TCI device [14]. TCI using the MH induces immune responses against ovalbumin and adenovirus vector, with an efficacy comparable to that of injected vaccination systems [14]. In the present study, we investigated the vaccination efficacy of our TCI system for practical infectious disease models, which is essential for validating

Abbreviations: Ag, antigen; APC, antigen-presenting cell; BSA, bovine serum albumin; CT, cholera toxin; DT, diphtheria toxoid; HA, hemagglutinin; HI, hemagglutination inhibition; IDI, intradermal immunization; IMI, intramuscular immunization; MH, MicroHyal; PBS, phosphate-buffered saline; RBC, red blood cell; SCI, subcutaneous immunization; TCI, transcutaneous immunization; TT, tetanus toxoid.

* Corresponding author. Tel./fax: +81 6 6879 8176.

** Corresponding author. Tel.: +81 6 6879 8175; fax: +81 6 6879 8179.

E-mail addresses: okada@phs.osaka-u.ac.jp (N. Okada), nakagawa@phs.osaka-u.ac.jp (S. Nakagawa).

the use of this TCI system. We examined the potential advantage of the TCI system using tetanus toxoid (TT), diphtheria toxoid (DT), SE36, and influenza hemagglutinin (HA) as Ags. In addition, we compared the vaccination efficacy of our TCI system to that of conventional immunization systems, such as subcutaneous immunization (SCI), intradermal immunization (IDI), intramuscular immunization (IMI), and intranasal immunization (INI), which is a recently introduced method of administering attenuated influenza vaccine via the nasal cavity. Our findings revealed that our TCI system induced an immune response that provides excellent protection against infectious diseases. Based on these results, we are continuing our studies to facilitate the application of this vaccination system using MH for clinical use as a simple, easy-to-use, and effective vaccination method to provide infectious disease prophylaxis.

2. Materials and methods

2.1. Animals

Female BALB/c mice (6 weeks old), ICR mice (6 weeks old), and hairless rats (5 weeks old) were purchased from SLC Inc. (Hamamatsu, Japan). All animals were specific pathogen free and maintained in the experimental animal facility at the Osaka University. The experiments were conducted in accordance with the guidelines provided by the Animal Care and Use Committee of Osaka University. Our permit number for this study is “doyaku23-3-0”.

2.2. Ags

TT, DT, SE36 [15], seasonal trivalent influenza HA from each of A/Brisbane/59/2007(H1N1), A/Uruguay/716/2007(H3N2), and B/Florida/4/2006, which were the influenza Ags recommended for inclusion for the 2007–2008 season, and influenza HA from mouse-adopted influenza virus A/PR/8/34 were kindly provided by the Research Foundation for Microbial Diseases of Osaka University, Suita, Japan.

2.3. MH fabrication

Sodium hyaluronate was dissolved in distilled water, and then Ags were added and uniformly mixed. The aqueous solution was cast into micromolds and dried in a desiccator at room temperature. MHs were obtained by separating them from the molds. MHs were either 300 μm (MH300) or 800 μm (MH800) high, and contained over 200 microneedles/ cm^2 . To form the microneedle patch system, arrays with an area of 0.8 cm^2 were fixed onto an adhesive film with a surface area of 2.3 cm^2 .

2.4. Vaccination protocol

2.4.1. TT/DT vaccination

Combined TT and DT-containing MH300 (1 or 3 μg each) and MH800 (0.1, 1, or 10 μg each) were applied onto the back skin of hairless rats for 6 h. Control SCI groups were subcutaneously immunized with combined TT and DT (10 μg each). These procedures were repeated five times at 2-week intervals. At the indicated periods, sera were collected from the rats to determine the toxoid-specific IgG titer, and sera collected 2 weeks after last vaccination were assayed for analysis of the IgG subclass and the passive challenge experiment described below.

2.4.2. SE36 vaccination

SE36-containing MH300 (0.1 or 2 μg) and MH800 (0.1 or 2 μg) were applied onto the shaved back skin of BALB/c mice for 6 h. In the SCI group, BALB/c mice were subcutaneously injected with SE36 (0.1 or 5 μg). These procedures were repeated four times at 2-week intervals. At the indicated periods, sera were collected from the mice to determine the toxoid-specific IgG titer, and sera collected

2 weeks after the last vaccination were assayed for analysis of IgG subclass and immunofluorescence assay as described below.

2.4.3. Influenza HA vaccination

For the seasonal trivalent influenza vaccination, three influenza HA-containing MH800 (0.2 μg each) were prepared. The MHs were applied to the shaved back skin of BALB/c for 6 h. For the control groups, BALB/c mice were treated by either IMI or IDI with three HAs (0.2 μg each) alone or with alum (100 μg), or by INI with three HAs (0.2 μg each) alone or with 10 μg cholera toxin (CT). These procedures were repeated twice at 4-week intervals. At the indicated periods, sera were collected from the mice to determine the HA-specific IgG titer. Sera collected 2 weeks after the last vaccination were assayed for analysis of IgG subclass and HI titer measurement.

For the live influenza virus challenge experiment, HA from mouse-adopted A/PR8/34 (0.4 μg)-containing MH800 was used. Control IMI or INI groups were treated with intramuscular injection of HA (0.4 μg) and intranasal application of HA (0.4 μg), respectively, plus CT (10 μg). The non-immunized group received Ag-free MH800. These procedures were repeated twice at 4-week intervals. At the indicated periods, sera were collected from the mice to determine the HA-specific IgG titer. Sera collected 2 weeks after the last vaccination were assayed for analysis of IgG subclass and HI titer measurement.

2.5. Antibody titer measurement

Serum was collected from animals at the indicated time-points, and the Ag-specific IgG or IgG subclass titer was determined by ELISA following previously described protocols [16]. End-point titers of Ag-specific antibody were expressed as the reciprocal \log_2 of the last dilution that showed 0.1 absorbance units after subtracting the background.

2.6. Passive challenge experiment for tetanus toxin

Neutralization activity of test sera collected from hairless rats that had been vaccinated five times with TT and DT was evaluated following previously described protocols [16]. Two weeks after the final vaccination, test sera were collected from hairless rats that had been vaccinated five times with TT and DT. ICR mice were injected subcutaneously with a 50- μl mixture of 25- μl test serum diluted at 1/1, 1/10, 1/100, 1/1000, and 25- μl solution containing 20 ng tetanus toxin (Sigma-Aldrich, Inc., St. Louis, MO) after incubation at 37 $^\circ\text{C}$ for 1 h. Mice were monitored for survival every 3 h for 96 h.

2.7. Immunofluorescence assays

Sera collected 2 weeks after the last vaccination of SE36 were assayed for analysis of immunofluorescence assay as described below. Percoll-purified red blood cells (RBC) infected by trophozoites and schizonts were prepared following the previously described protocol [17]. The RBCs were fixed with 3% paraformaldehyde/phosphate-buffered saline (PBS) for 20 min at 4 $^\circ\text{C}$, centrifuged at 1870 g for 10 min at 4 $^\circ\text{C}$, and resuspended in 3% bovine serum albumin (BSA; Sigma-Aldrich)/PBS. The fixed RBCs were dropped onto slide glass and dried at room temperature for 10 min. Then, 1% Triton X-100 in PBS was added, the plates were placed at room temperature for 1 h and then washed with PBS three times. The RBCs were blocked with 3% BSA/PBS for 1 h at room temperature. After washing twice with PBS, serum diluted 1:100 with 3% BSA/PBS was added to RBCs and incubated for 1 h at room temperature. The RBCs were washed five times with PBS and Alexa Fluor 488-conjugated anti-mouse IgG antibody (20 $\mu\text{g}/\text{ml}$; Invitrogen, Carlsbad, CA) was added. After 1 h incubation at room temperature, the RBCs were washed with PBS five times and mounted with Prolong Gold anti-fade reagent with 4',6-diamidino-2-phenylindole (Invitrogen).

2.8. Hemagglutination inhibition (HI) titer measurement

In influenza vaccination, sera collected 2 weeks after the last vaccination were assayed for analysis of HI titer measurement following established protocols. Briefly, sera were treated with receptor-destroying enzyme (DENKA SEIKEN Co., Ltd., Tokyo, Japan) at 37 °C overnight according to the manufacturer's instructions. After treatment, 25- μ l aliquots of 2-fold serially diluted serum were incubated with 25 μ l of 4 HA units of each HA at 37 °C for 1 h, followed by incubation with 50 μ l of 0.5% chicken RBC (Nippon Biotest Laboratories Inc., Tokyo, Japan) at 25 °C for 45 min. The HI titer was defined as the reciprocal of the highest serum dilution that inhibited hemagglutination.

2.9. Influenza virus challenge

The live influenza virus challenge was conducted at Japan Biological Science (Osaka, Japan). Two weeks after the last vaccination, mice were challenged by intranasal instillation of 5×10^6 PFU of mouse-adapted influenza virus A/PR/8/34. After that, mice were monitored for weight loss and signs of illness on a daily basis and evaluated as described in Supplementary Table 1. Six days after the challenge, the lungs were collected to determine the degree of lung consolidation based on the following scale: 1, no consolidation; 2, $\leq 1/3$ lobe; 3, $> 1/3$ to $\leq 1/2$ lobe; 4, $> 1/2$ to $\leq 2/3$ lobe; and 5, $> 2/3$ lobe, to measure the virus plaque using a plaque assay system, and to perform a histopathologic assessment by hematoxylin and eosin staining. Inflammation level of bronchial pneumonia and interstitial pneumonia was scored according to severity, as follows: 0, none; 1, very slight; 2, mild; 3, moderate; and 4, severe. In addition, the pneumonia was categorized as bronchopneumonia or interstitial pneumonia as follows: bronchopneumonia; hypertrophy of bronchus mucous epithelium, hyperplasia of bronchus mucous epithelium, denaturation or necrosis of bronchus mucous epithelium, and infiltration with mononuclear cells and polymorphonuclear neutrophil leukocyte of bronchial submucosa. Interstitial pneumonia; focal atelectic lung or alveolus of the lung, focal hydrops or alveolus of the lung, focal bleed or alveolus of the lung, infiltration with mononuclear cells and polymorphonuclear neutrophil leukocyte of alveolar septum and infiltration with mononuclear cells and polymorphonuclear neutrophil leukocyte of alveolus of the lung.

3. Results

3.1. Efficacy of TT/DT vaccination

We examined the vaccination efficacy of our TCI system for TT and DT as typical clinical vaccine Ags. Hairless rats vaccinated by TCI using MH800 had an increased anti-TT IgG titer after the first vaccination at a low Ag dose, which was comparable to that of the SCI groups (Fig. 1A, B). The anti-DT IgG titer increased following vaccination using either MH800 or SCI, and this effect was dose-dependent. In the TCI group using MH300, the anti-TT or DT IgG titer increased with the increasing number of vaccinations, and achieved maximum levels equivalent to the MH800 and SCI groups (Fig. 1C, D). With the MH800, the anti-DT IgG titer was dose-dependent, suggesting that TT had high antigenicity. To evaluate the Th1/Th2 immune balance in our TCI system, we analyzed the toxoid-specific IgG subclass (Fig. 1E, F). Among the rat IgG subclasses, IgG1 and IgG2a are classified as Th2-dependent, and IgG2c as Th1-dependent [18]. SCI group induced IgG1, IgG2a, and IgG2c. On the other hand, TCI using MH300 or MH800 induced mainly IgG1 and IgG2a, but not IgG2c. Thus, our TCI system elicited a Th2-type immune response rather than a Th1-type. In a passive-challenge experiment, all mice treated with serum from non-immunized rats died (Table 1). On the other hand, 4 of 4 test sera (1/100 dilution) from rats vaccinated by TCI using MH800 with combined TT and DT (10 μ g each) neutralized the tetanus toxin, and this activity was also observed in TCI

group using MH800 (0.1 or 1 μ g each). In the TCI group using MH300, 1 of 4 test sera (1/100 dilution), or 2 of 4 test sera (1/10 dilution) neutralized the tetanus toxin. These results indicated that our TCI system using each MH type induced toxoid-specific neutralization antibody and blocked the development of infection.

3.2. Efficacy of SE36 vaccination

We examined whether anti-SE36 IgG was produced by our TCI system. In mice vaccinated by TCI using MH800, anti-SE36 IgG increased in a dose-dependent manner equivalent to that in SCI group (Fig. 2A). TCI using MH300 containing 2 μ g SE36 induced SE36-specific IgG production equivalent to TCI using MH800 and SCI, but achieving the maximum IgG

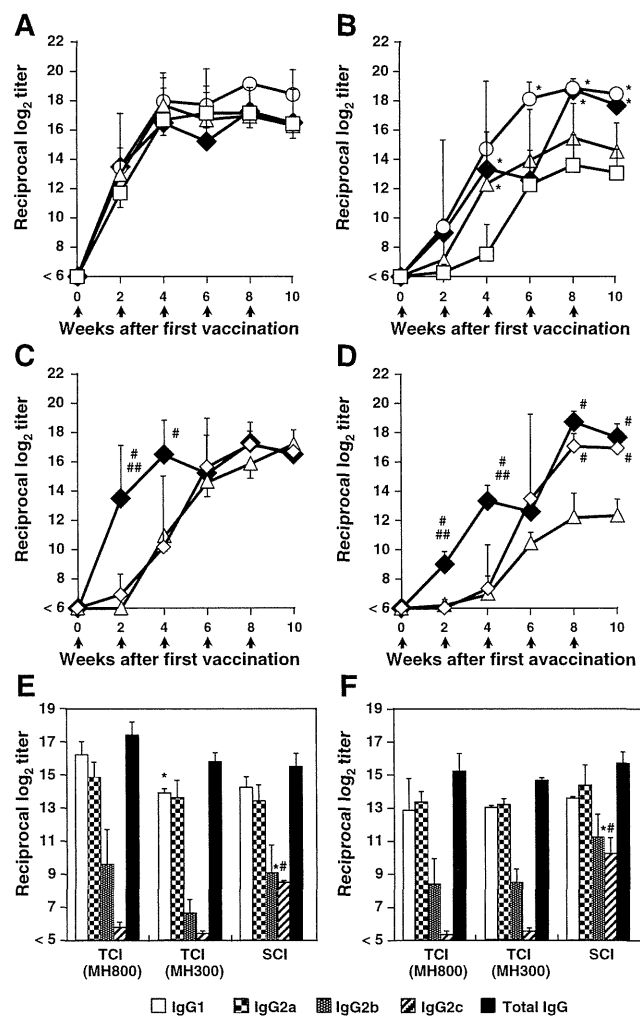


Fig. 1. Toxoid-specific IgG antibody responses after TCI. Combined TT and DT-containing (A,B) MH800 (0.1 mg; \square , 1 mg; \triangle , or 10 mg; \bullet each), or (C,D) MH300 (1 mg; \square , or 3 mg; \triangle each) were applied to the back skin of hairless rats for 6 h five times at 2-week intervals. As a control SCI group (\square), hairless rats were injected with combined TT and DT (10 mg each). At the indicated points, sera collected from these hairless rats were assayed for the IgG titer to TT (A, C) or DT (B, D) by ELISA. Two weeks after the final vaccination, sera collected from rats transcutaneously vaccinated using MH800 containing both TT and DT (10 mg each) or MH300 (3 mg each), and immunized subcutaneously with combined TT and DT (10 mg each) were assayed for TT (E) or DT (F)-specific IgG subclass (IgG1, IgG2a, IgG2b, or IgG2c) titer by ELISA. Data are expressed as mean \pm SE of results from 3–4 rats. Arrowhead indicates vaccination points. Statistical significance was evaluated by one-way analysis of variance followed by Tukey's test for multiple comparisons. (A, B) *; $p < 0.01$ versus TCI (MH800/0.1 mg) group. (C,D) #; $p < 0.01$ versus TCI (MH300/1 mg) group. ##; $p < 0.01$ versus TCI (MH300/3 mg) group. (E,F) *; $p < 0.01$ versus TCI (MH800) group. #; $p < 0.01$ versus TCI (MH300) group.

Table 1
Passive-challenge experiment of mice with tetanus toxin.^a

Vaccination			Survival ratio		
Route	Device	Toxoid ($\mu\text{g}/\text{site}$)	1/1 ^b	1/10 ^b	1/100 ^b
TCI	MH800	10 μg each	4/4	4/4	4/4
TCI	MH800	1 μg each	3/3	3/3	2/3
TCI	MH800	0.1 μg each	4/4	4/4	2/4
TCI	MH300	3 μg each	4/4	4/4	1/4
TCI	MH300	1 μg each	4/4	2/4	0/4
SCI	Injection	10 μg each	4/4	4/4	3/4

^a Test sera were collected 2 weeks after the final vaccination from hairless rats that were vaccinated 5 times at 2-week intervals. The mice were injected subcutaneously with a 50- μl mixture of the indicated dilutions of test sera and 20 ng tetanus toxin after incubating the mixture at 37 °C for 1 h.

^b Dilution ratio of test sera.

titer level required additional vaccinations. Next, we investigated whether the anti-SE36 IgG antibody binds to the malaria parasite. An immunofluorescence assay in the TCI and SCI groups detected green fluorescence derived from SE36-specific IgG in the same region of the blue

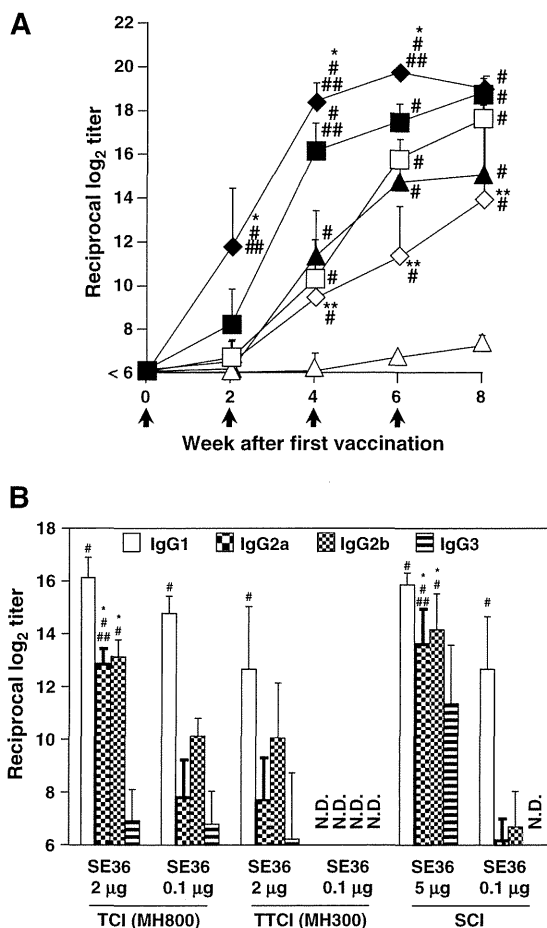


Fig. 2. SE36-specific IgG antibody responses after TCI. SE36-encapsulated MH800 (0.1 mg; ϵ , or 2 mg; ζ) or MH300 (0.1 mg; r , or 2 mg; p) was applied to back skin of BALB/c mice for 6 h four times at 2-week intervals. As a control group, BALB/c mice were subcutaneously injected with SE36 (0.1 mg; τ , or 5 mg; ζ). (A) At the indicated points, sera collected from these mice were assayed for the IgG titer to SE36 by ELISA. (B) Two weeks after the final treatment, sera collected from these mice were assayed for SE36-specific IgG subclass (IgG1, IgG2a, IgG2b, or IgG3) titer by ELISA. Data are expressed as mean \pm SE of results from 5 mice. Arrowhead indicates vaccination points. Statistical significance was evaluated by one-way analysis of variance followed by Tukey's test for multiple comparisons. *, $p < 0.01$ versus TCI (MH800/0.1 mg) group. **, $p < 0.01$ versus TCI (MH800/2 mg) group. #, $p < 0.01$ versus TCI (MH300/0.1 mg) group. ##, $p < 0.01$ versus TCI (MH300/2 mg) group.

fluorescence produced by the malaria parasite, suggesting that the induced antibody binds to the malaria parasite (Fig. 3). Because other groups reported that IgG2a, IgG2b, and IgG3 among the IgG subclasses have important roles in the antiproliferative effect of malaria parasites [19], we analyzed the anti-SE36 IgG subclass. In TCI using MH300 containing 2 μg SE36 and MH800 containing 0.1 or 2 μg SE36, IgG1 was the main subclass, and IgG2a, IgG2b, and IgG3 were also produced (Fig. 2B). These results demonstrated that TCI using MH could induce an acquired immune response and provide adequate protection against malaria.

3.3. Efficacy of influenza HA vaccination

We compared the immune response induced by TCI using MH800 with that of the IMI, IDI, or INI groups. The results of the anti-HA IgG titer measurement (Fig. 4A–C) indicate that the IgG production profile in the TCI group was similar to that of IMI groups with or without alum as an adjuvant. The INI mice with HA alone produced a much lower anti-HA titer than the other groups. The IgG titer of the IDI mice with HA alone was also quite low. On the other hand, the anti-HA IgG titer increased in mice vaccinated by INI with HA plus CT or IDI with HA plus alum. Moreover, a sufficiently high IgG titer was still detected 16 weeks after the last vaccination, suggesting that the anti-HA IgG induced by the TCI system would remain effective throughout the duration of the flu season. In addition, we analyzed the HA-specific IgG subclass. Among the mouse IgG subclasses, IgG1 is classified as Th2-dependent, and IgG2a as Th1-dependent [20,21]. TCI with HAs had a similar IgG subclass pattern as the IMI and IDI groups, whereas the INI group had greater induction of the Th1-type IgG subclass (IgG2a) than the other vaccinated groups (Fig. 4D–F). We then analyzed the HI titer of sera as the serological measure of

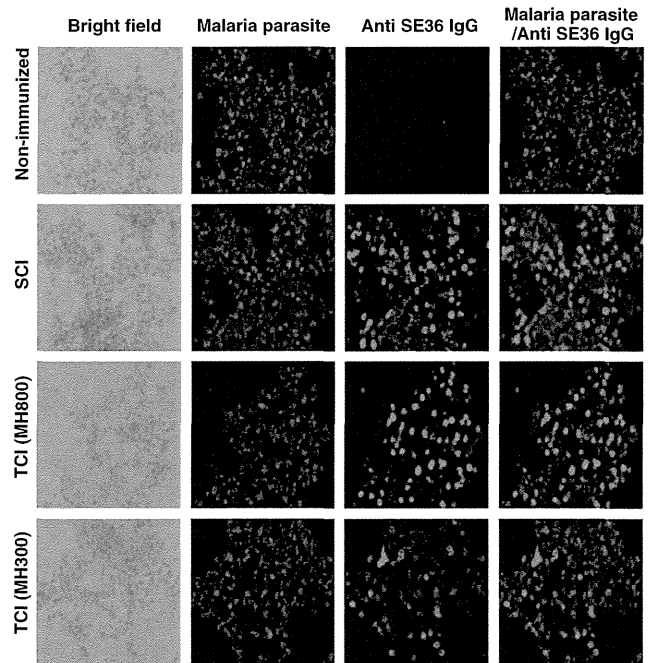


Fig. 3. Fluorescence microscopic analysis of antibody-binding activity. BALB/c mice were transcutaneously vaccinated with SE36 (2 $\mu\text{g}/\text{MH300}$) or (2 $\mu\text{g}/\text{MH800}$) for 6 h four times at 2-week intervals. A control group was subcutaneously injected with SE36 (5 μg) four times at 2-week intervals. Two weeks after the final treatment, sera were collected from these mice. Trophozoite- and schizont (CDC1)-infected erythrocytes were identified in the sera. Anti-SE36 antibody binding to CDC1-infected erythrocytes was stained with Alexa Fluor 488-conjugated goat anti-mouse IgG antibody. The nucleus was counterstained using 4',6-diamidino-2-phenylindole, and then CDC1-infected erythrocytes were photographed under a fluorescence microscope. TCI; transcutaneous immunization, SCI; subcutaneous immunization.

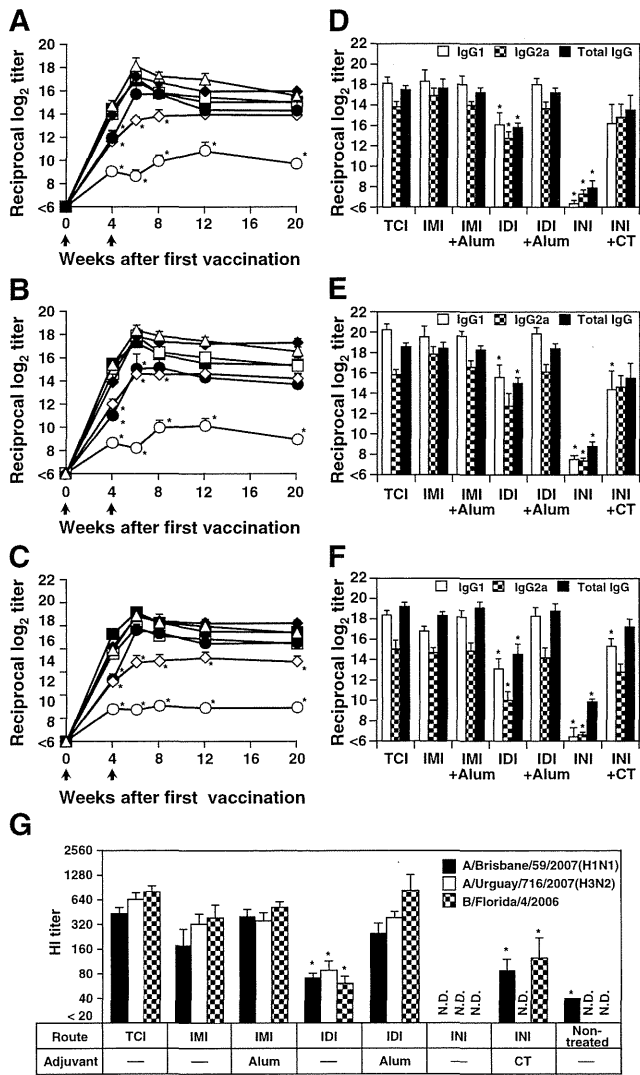


Fig. 4. Anti-HA immune responses in BALB/c mice after TCI. BALB/c mice were transcutaneously vaccinated with trivalent seasonal influenza HA from [(A,D) A/Brisbane/59/2007 (H1N1), (B,E) A/Uruguay/716/2007 (H3N2), and (C,F) B/Florida/4/2006] (0.2 mg each; r) for 6 h twice at 4-week intervals. Control groups were treated with intramuscular (E), intradermal (I), or intranasal (I) application of HAs (each 0.2 mg) twice at 4-week intervals. Another control group was treated with intramuscular injection of HA Ags (each 0.2 mg) with alum (100 mg) (c), intradermal application of HA Ags (each 0.2 mg) combined with alum (100 mg) (l), or intranasal application of HA Ags (each 0.2 mg) with CT (10 mg) (i) twice at 4-week intervals. (A–C) At the indicated points, sera collected from these mice were assayed to determine the HA-specific IgG titer by ELISA. (D–F) Sera collected 2 weeks after the last treatment were assayed for HA-specific IgG subclass (IgG1 and IgG2a) by ELISA. (G) Two weeks after the final treatment, sera collected from these mice were assayed for the HI titer. HI activity expressed as the highest dilution that resulted in complete inhibition of hemagglutination. Data are expressed as mean \pm SE of results from 5–7 mice. INI; intranasal immunization, IDI; intradermal immunization, N.D.; not detectable. Statistical significance was evaluated by one-way analysis of variance followed by Tukey's test for multiple comparisons. *, $p < 0.01$ versus TCI (MH800) group.

functional antibodies. HI activity of TCI group was comparable to that in the IMI and IDI groups (combined with alum), and the levels appeared to correlate with the levels of anti-HA IgG antibody response (Fig. 4G). On the other hand, the IDI group (without alum) and INI group had lower HI activity than the TCI group. INI (with CT) induced high HA-specific IgA production which has a critical role in protecting against infection, whereas little anti-HA IgA was detected in the other vaccination groups, suggesting that our TCI system could not induce an HA-specific

IgA response to the same extent as the conventional injection system (Supplementary Fig. 1). The results presented above indicate that TCI using MH induced strong antibody responses with significant HI titers.

In virus challenge experiment, TCI elicited HA-specific functional IgG antibody equivalent to that in the IMI and INI groups (Fig. 5A–C), whereas little anti-HA IgA antibody was detected in the TCI and IMI groups (Supplementary Fig. 2). After A/PR/8/34 influenza virus challenge, control mice treated with Ag-free MH800 (MH800/placebo)

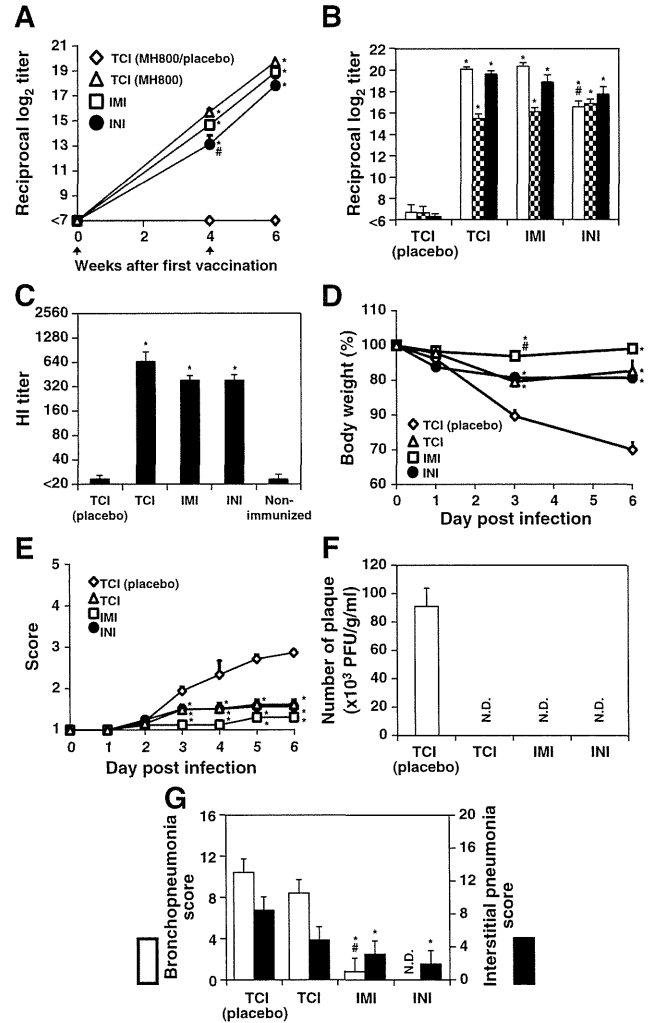


Fig. 5. Protection of vaccinated mice against influenza virus challenge. BALB/c mice were transcutaneously vaccinated with HA from [A/PR/8/34 (H1N1)] (0.4 mg) for 6 h twice at 4-week intervals. Control groups were treated with transcutaneous application without HA, intramuscular injection of HA (0.4 mg), or intranasal application of HA (0.4 mg) combined with CT (10 mg) twice at 4-week intervals. These mice were each infected intranasally with 6×10^5 PFU of the A/PR/8/34(H1N1) virus. (A) At the indicated points, sera collected from these mice were assayed for the HA-specific IgG titer by ELISA. (B,C) Two weeks after the final treatment, sera collected from these mice were assayed for (B) anti-HA IgG subclass (IgG1 and IgG2a) and (C) the HI titer. HI activity is expressed as the highest dilution that resulted in complete inhibition of hemagglutination. Data are expressed as mean \pm SE of results from 13 mice. (D) Body weight was measured each day and is presented as a percentage of the original weight before infection (day 0). (E) The performance status of the mice was scored every day. (F) Six days after infection, the lungs were collected from these mice and number of viruses in the lung homogenate was determined using a plaque assay system. (G) The degree of inflammation of the lung was scored as follows: 0, none; 1, very slight; 2, mild; 3, moderate; and 4, severe. Pathologic findings were classified into bronchopneumonia and interstitial pneumonia. (D–G) Data are expressed as mean \pm SE of results from 10 mice. Statistical significance was evaluated by one-way analysis of variance followed by Tukey's test for multiple comparisons. *, $p < 0.01$ versus TCI (MH800/placebo) group. #, $p < 0.01$ versus TCI (MH800) group.

Table 2
Degree of lung consolidation.

Vaccination	Lung weight (g; mean \pm SE)		Consolidation (/tested mice)				Score (mean \pm SE) ^a	
	L ^b	R ^b	L ^b	R ^b	R&L ^b	No	L ^b	R ^b
TCl (placebo)	0.154 \pm 0.007	0.243 \pm 0.022	1	0	9	0	4.2 \pm 0.2	3.4 \pm 0.5
TCl	0.068 \pm 0.007	0.142 \pm 0.013	0	1	0	9	1.0 \pm 0.0	1.1 \pm 0.1
IMI	0.059 \pm 0.003	0.123 \pm 0.005	0	0	0	10	1.0 \pm 0.0	1.0 \pm 0.0
INI	0.057 \pm 0.002	0.117 \pm 0.003	0	0	0	10	1.0 \pm 0.0	1.0 \pm 0.0

^a Degree of consolidation: 1; no consolidation, 2; \leq 1/3 lobe, 3; $>$ 1/3 to \leq 1/2 lobe, 4; $>$ 1/2 to \leq 2/3 lobe, and 5; $>$ 2/3 lobe.

^b L: left lobe, R: right lobe, R&L: right and left lobes.

succumbed; they lost 30% of their body weight and showed worsening of symptoms (Fig. 5D, E). In contrast, TCl group mice showed no remarkable weight loss or other symptoms of illness, similar to the IMI and INI groups. In MH800/placebo group mice, influenza virus was detected at 10^5 plaque forming units (PFU)/g/ml, but the virus titer in the lungs of the TCl group was below the detection limit, demonstrating that our TCl system provided protection equal to that of IMI and INI (Fig. 5F). The weight of lungs harvested from mice vaccinated by TCl was equal to that of the IMI and INI groups. In the macroscopic findings, consolidation was not observed in 9/10 of the TCl group, 10/10 of the IMI group, and 10/10 of the INI group (Table 2). On the other hand, in the non-immunized group, lung weight was much greater than in the other groups and consolidation was detected in all of the mice. Based on our evaluation of the degree of bronchial pneumonia and interstitial pneumonia, the TCl group had a tendency toward a lower degree of lung inflammation compared with the non-immunized group, and the inflammation score in the IMI and INI groups was significantly lower (Fig. 5G). On the basis of these results, our TCl system confers protective immunity as effectively as IMI and INI administrations.

4. Discussion

We developed a novel TCl system using dissolving microneedle arrays, comprising MHs. This study demonstrated the vaccination efficacy of our TCl system against tetanus and diphtheria, malaria, and influenza as practical infection models.

TCl using MH without adjuvant induced effective immune responses as well as IMI, IDI, and SCI, indicating that this TCl system can replace the conventional injection system. INI system is attractive because it can induce the mucosal immune responses based on IgA production. Unfortunately, in this study, our TCl system did not induce the HA-specific IgA. Other reports showed that TCl system combining with some adjuvants such as CT, heat-labile toxin, or CpG could induce mucosal immune responses [22,23]. Therefore, we are currently exploring adjuvant candidates for our TCl system to improve our TCl system such as induction of mucosal immunity or cellular immunity.

In a previous report [24] on TCl using a hydrogel patch containing TT and DT, 100 μ g each of TT and DT was needed to induce the maximum effect. Our TCl system using MH induced the same maximal effect with a lower Ag dose; 1/100–1/1000 as compared with that of a hydrogel patch, suggesting that the TCl system using MH is superior to that using a hydrogel patch in terms of Ag dose reduction. We also investigated whether TCl using a hydrogel patch containing SE36 induced SE36-specific IgG antibody production, and the results showed that TCl using a hydrogel patch with or without adjuvant did not induce anti-SE36 IgG production (Supplementary Fig. 3). Moreover, TCl using MH effectively induced immune responses against particulate Ags, like influenza HA. Based on these results, TCl using MH represents a significant advance over previous TCl approaches.

There were difference in strength of Ag-specific antibody production induced by TCl using MH300 and MH800 in TT/DT or SE36 vaccination. This distinct immune response seemed to be due to differences in the Ag-presenting cell (APC) subset involved in Ag capture. Additionally,

based on the IgG subclass analysis, TCl using MH induced a greater Th2-dominant immune response than the injection system in TT/DT vaccination, but almost the same IgG subclass pattern as the injection system in influenza vaccination. The detailed mechanism underlying the immune responses or Th1/Th2 balance is unknown. APCs are thought to have an important role in controlling the characteristics of immune responses, and therefore we are now investigating the characteristics of the immune response in Lang-DTR-EGFP mice [25] or CD11c-DTR-EGFP mice [26], in which the Langerhans cells or CD11c-positive cells can be depleted by intraperitoneal injection of diphtheria toxin to study the role of APCs in our TCl system. Evaluation of the impact of our TCl using MH300 and MH800 on the strength of immune responses and Th1/Th2 balance in animals will help to define the characteristics of the TCl system, and to determine additional applications of our TCl system.

5. Conclusion

The findings of our present study indicate that our TCl system using MH induced effective immune responses against infectious diseases. For clinical application of this TCl system, we are planning translational studies and manufacturing methods for the TCl formulation must also be established. We expect that our vaccine delivery technology will lead to the launch of a TCl system that is efficacious, easy-to-use, cost-effective, and widely acceptable to the public.

Supplementary data related to this article can be found online at <http://dx.doi.org/10.1016/j.jconrel.2012.04.001>.

Acknowledgment

This work was supported by the Program for Promotion of Fundamental Studies in Health Sciences of the National Institute of Biomedical Innovation (NIBIO), by Health Labour Sciences Research Grant from the Ministry of Health, Labour and Welfare, and by Grant-in-Aid for Scientific Research (B) (24390041) from the Ministry of Education, Culture, Sports, Science, and Technology of Japan.

References

- [1] J. Cohen, M. Enserink, Swine flu. After delays WHO agree: the 2009 pandemic has begun, *Science* 324 (2009) 1496–1497.
- [2] C. Fraser, C.A. Donnelly, S. Cauchemez, W.P. Hanage, M.D. Van Kerkhove, T.D. Hollingsworth, J. Griffin, R.F. Baggaley, H.E. Jenkins, E.J. Lyons, T. Jombart, W.R. Hinsley, N.C. Grassly, F. Balloux, A.C. Ghani, N.M. Ferguson, A. Rambaut, O.G. Pybus, H. Lopez-Gatell, C.M. Alpujch-Aranda, I.B. Chapela, E.P. Zavala, D.M. Guevara, F. Checchi, E. Garcia, S. Hugonnet, C. Roth, Pandemic potential of a strain of influenza A (H1N1): early findings, *Science* 324 (2009) 1557–1561.
- [3] A.J. Tatem, D.L. Smith, P.W. Gething, C.W. Kabaria, R.W. Snow, S.I. Hay, Ranking of elimination feasibility between malaria-endemic countries, *Lancet* 376 (2010) 1579–1591.
- [4] R. Romi, D. Boccolini, S. D'Amato, C. Cenci, M. Peragallo, F. D'Ancona, M.G. Pompa, G. Majori, Incidence of malaria and risk factors in Italian travelers to malaria endemic countries, *Travel Med. Infect. Dis.* 8 (2010) 144–154.
- [5] E.L. Giudice, J.D. Campbell, Needle-free vaccine delivery, *Adv. Drug Deliv. Rev.* 58 (2006) 68–89.
- [6] N. Azad, Y. Rojanasakul, Vaccine delivery—current trends and future, *Curr. Drug Deliv.* 3 (2006) 137–146.
- [7] M.M. Levine, Can needle-free administration of vaccines become the norm in global immunization? *Nat. Med.* 9 (2003) 99–103.

- [8] G.M. Glenn, T. Schariton-Kersten, C.R. Alving, Advances in vaccine delivery: transcutaneous immunisation, *Expert Opin. Investig. Drugs* 8 (1999) 797–805.
- [9] P. Chiarella, V.M. Fazio, E. Signori, Application of electroporation in DNA vaccination protocols, *Curr. Gene Ther.* 10 (2010) 281–286.
- [10] P. Batheja, R. Thankur, B. Michniak, Transdermal iontophoresis, *Expert Opin. Drug Deliv.* 3 (2006) 127–138.
- [11] J. Baxter, S. Mitragotri, Needle-free liquid jet injections: mechanisms and applications, *Expert Rev. Med. Devices* 3 (2006) 565–574.
- [12] D.V. McAllister, P.M. Wang, S.P. Davis, J.H. Park, P.J. Canatella, M.G. Allen, M.R. Prausnitz, Microfabricated needles for transdermal delivery of macromolecules and nanoparticles: fabrication methods and transport studies, *Proc. Natl. Acad. Sci. U. S. A.* 100 (2003) 13755–13760.
- [13] S.P. Sullivan, D.G. Koutsonanos, M. Del Pilar Martin, J.W. Lee, V. Zarnitsyn, S.O. Choi, N. Murthy, R.W. Compans, I. Skountzou, M.R. Prausnitz, Dissolving polymer micro-needle patches for influenza vaccination, *Nat. Med.* 16 (2010) 915–920.
- [14] K. Matsuo, Y. Yokota, Y. Zhai, Y.S. Quan, F. Kamiyama, Y. Mukai, N. Okada, S. Nakagawa, A low-invasive and effective transcutaneous immunization system using a novel dissolving microneedle array for soluble and particulate antigens, *J. Control. Release* (in press).
- [15] T. Horii, H. Shirai, L. Jie, K.J. Ishii, N.Q. Palacpac, T. Tougan, M. Hato, N. Ohta, A. Bobogare, N. Arakaki, Y. Matsumoto, J. Namazue, T. Ishikawa, S. Ueda, M. Takahashi, Evidences of protection against blood-stage infection of *Plasmodium falciparum* by the novel protein vaccine SE36, *Parasitol. Int.* 59 (2010) 380–386.
- [16] K. Matsuo, Y. Ishii, Y.S. Quan, F. Kamiyama, Y. Mukai, Y. Yoshioka, N. Okada, S. Nakagawa, Transcutaneous vaccination using a hydrogel patch induces effective immune responses to tetanus and diphtheria toxoid in hairless rat, *J. Control. Release* 149 (2011) 15–20.
- [17] T. Sugiyama, K. Suzue, M. Okamoto, J. Inselburg, K. Tai, T. Horii, Production of recombinant SERA proteins of *Plasmodium falciparum* in *Escherichia coli* by using synthetic genes, *Vaccine* 14 (1996) 1069–1076.
- [18] J. Binder, E. Graser, W.W. Hancock, B. Wasowska, M.H. Sayegh, H.D. Volk, J.W. Kupiec-Weglinski, Downregulation of intragraft IFN-gamma expression correlates with increased IgG1 alloantibody response following intrathymic immunomodulation of sensitized rat recipients, *Transplantation* 60 (1995) 1516–1524.
- [19] N.C. Smith, L. Favila-Castillo, A. Monroy-Ostria, C. Hirunpetcharat, M.F. Good, The spleen, IgG antibody subsets and immunity to *Plasmodium berghei* in rats, *Immunol. Cell Bio.* 75 (1997) 318–323.
- [20] F.D. Finkelman, I.M. Katona, T.R. Mosmann, R.L. Coffman, IFN- γ regulates the isotypes of Ig secreted during in vivo humoral immune responses, *J. Immunol.* 140 (1988) 1022–1027.
- [21] S. Bergstedt-Lindqvist, H.B. Moon, U. Persson, G. Möller, C. Heusser, E. Severinson, Interleukin 4 instructs uncommitted B lymphocytes to switch to IgG1 and IgE, *Eur. J. Immunol.* 18 (1988) 1073–1077.
- [22] I.M. Belyakov, S.A. Hammond, J.D. Ahlers, G.M. Glenn, J.A. Berzofsky, Transcutaneous immunization induces mucosal CTLs and protective immunity by migration of primed skin dendritic cells, *J. Clin. Invest.* 113 (2004) 998–1007.
- [23] G.M. Glenn, C.P. Villar, D.C. Flver, A.L. Bourgeois, R. McKenzie, R.M. Lavker, S.A. Frech, Safety and immunogenicity of an enterotoxigenic *Escherichia coli* vaccine patch containing heat-labile toxin: use of skin pretreatment to disrupt the stratum corneum, *Infect. Immun.* 75 (5) (2007) 2163–2170.
- [24] K. Matsuo, Y. Ishii, Y.S. Quan, F. Kamiyama, Y. Mukai, Y. Yasuo, N. Okada, S. Nakagawa, Transcutaneous vaccination using a hydrogel patch induces effective immune responses to tetanus and diphtheria toxoid in hairless rat, *J. Control. Release* 149 (2011) 15–20.
- [25] A. Kissenpennig, S. Henri, B. Dubois, C. Laplace-Builhé, P. Perrin, N. Romani, C.H. Tripp, P. Douillard, L. Leserman, D. Kaiserlian, S. Saeland, J. Davoust, B. Malissen, Dynamics and function of Langerhans cells in vivo: dermal dendritic cells colonize lymph node areas distinct from slower migrating Langerhans cells, *Immunity* 22 (2005) 643–654.
- [26] S. Jung, D. Unutmaz, P. Wong, G. Sano, K. De los Santos, T. Sparwasser, S. Wu, S. Vuthoori, K. Ko, F. Zavala, E.G. Pamer, D.R. Littman, R.A. Lang, In vivo depletion of CD11c⁺ dendritic cells abrogates priming of CD8⁺ T cells by exogenous cell-associated antigens, *Immunity* 17 (2002) 211–220.



総説

経皮ワクチンの進歩と展望*

廣部 祥子** 岡田 直貴** 中川 晋作**

Key Words : transcutaneous vaccination, hydrogel patch, self-dissolving microneedle array, clinical study

はじめに

1980年のWHOによる天然痘根絶宣言がワクチン開発の成果であるように¹⁾, 感染症対策においてワクチンが果たしてきた功績は輝かしいものである。しかしながら, 実用化ワクチンの大半を占める注射型ワクチンは, その施行に医療技術者を必要とし, 注射剤の輸送・保管に一貫した低温温度管理(コールドチェーン)が不可欠であるなど, 経済的・技術的な制約によって予防接種を最も必要とする地域へのワクチン普及を停滞させている。また, 新興・再興感染症の世界的流行やバイオテロリズム発生時に, ワクチンの大規模投与を迅速に実施できない点も懸念されている。

このような背景の下, 医療技術者や注射針などの医療器具を必要としない簡便なワクチン手法として, 「飲むワクチン」「吸うワクチン」「貼るワクチン」などの開発が精力的に行われている。その中で著者らは, 皮膚に貼るだけで感染症に対する防御効果を獲得可能な経皮ワクチン製剤「貼るワクチン」の実用化を目指している。

本総説では, これまでの経皮ワクチン用デバイスの進歩を概説するとともに, 著者ら独自のデバイスである親水性ゲルパッチならびに皮膚内溶解型マイクロニードルの研究成果を通して, 経皮ワクチンの今後の展望を述べる。

経皮ワクチンデリバリー技術の発展

皮膚は, 生体と外界を隔てる組織であり, 常に異物侵入の危険に曝されている。そのため, 皮膚内には, 免疫監視機構において非常に重要な役割を担う抗原提示細胞(APC)が豊富に存在する(図1)。このように皮膚は, 生体の防御機能が高度に発達した「免疫学的バリアー」を備えており, ワクチンのターゲットとして非常に優れた組織である。APCは, 異物を認識・捕食した後に免疫誘導の場である所属リンパ節へと遊走する。そして, T細胞ならびにB細胞を抗原特異的に活性化することで, 全身性の獲得免疫応答を誘導する。したがって, 貼るワクチンにおいて抗原特異的な免疫応答を強力に誘導するためには, 抗原を効率よくAPCの存在する生きた表皮・真皮に送達することが必要である。しかしながら, 皮膚の最外層には物質透過を防ぐ物理的バリアーとなる角質層が存在するため²⁾, ペプチドや蛋白質といった水溶性で高分子の抗原を単に皮膚表面に塗布するだけでは, 角質層下のAPCに抗原を効率よく送達することはできない。そこで, DDS領域で開発されてきた経皮薬物デリバリー技術を経皮抗原デリバリー技術として応用することで, APCの存在する生きた表皮・真皮にまで抗原を送達しうる「経皮ワクチンシステム」の開発が行われてきた。

* The advance and prospect of transcutaneous vaccination system.

** Sachiko HIROBE, Naoki OKADA, Ph.D. & Shinsaku NAKAGAWA, Ph.D.: 大阪大学大学院薬学研究科薬剤学分野 [〒565-0871 大阪府吹田市山田丘1-6]; Laboratory of Biotechnology and Therapeutics, Graduate School of Pharmaceutical Sciences, Osaka University, Suita, Osaka 565-0871, JAPAN

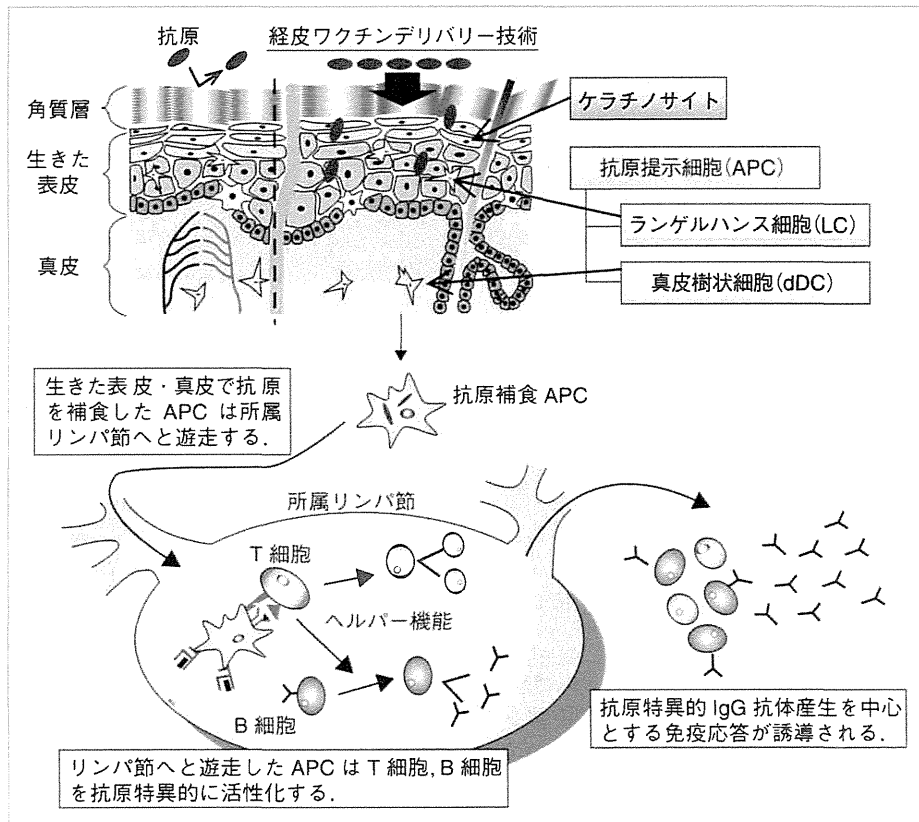


図1 経皮免疫誘導メカニズム

ケラチノサイト：各種サイトカインやケモカイン、増殖因子を分泌する。角質層下の生きた表皮の約90%を占めており、異物侵入に対する自然免疫の誘導にかかわっている。
 抗原提示細胞：抗原捕食によって、抗原特異的にリンパ球を感作する。ランゲルハンス細胞(LC)は生きた表皮に、真皮樹状細胞(dDC)は真皮に常在する。

具体例としては、皮膚への電圧負荷により一時的に角質層に孔をあけるエレクトロポレーション法³、電流負荷による水の移動とともにイオン性の物質を生きた表皮へと送達するイオントフォレシス法⁴、空気の圧力によって抗原を注入するJet injector⁵法などがあげられる。これらの手法によって確かに抗原が角質層を透過して生きた表皮にまで送達されることが実証されており、抗原特異的IgG抗体価の上昇が認められている。しかしこれらの方法は、特殊な装置を必要とすることから簡便性に乏しく、角質層を破壊してしまうことによる二次的な炎症や感染が危惧されるために、今のところ実用化までには至っていない。

そこで、まさに皮膚に貼るだけという簡便な

操作で抗原特異的な免疫応答を誘導できる粘着性パッチおよびガーゼパッチの研究開発が注目されている^{6,7}。しかしながら、これらの経皮ワクチン製剤は抗原を十分に浸透させるために、角質層あるいは角質層脂質成分を部分的に除去する前処理を必要とする。さらに、ガーゼパッチを応用した経皮ワクチン製剤は、皮膚に適用する直前に抗原溶液を浸み込ませるため、簡便性に欠けており、また注射型ワクチンと同様に抗原溶液の輸送や保管にコールドチェーンを必要とするなど、開発途上国へのワクチン普及を推し進めるためにはさらなる改良を加える必要がある。